Supporting Information

An Unsymmetrical Binuclear Iminopyridine-iron Complex and Its Catalytic Isoprene Polymerization†

Liang Wang,‡[a] Xiaowu Wang,‡[a] Hongbin Hou,[a] Guangqian Zhu,[a, b] Zhenyu Han,[a, b] Weiying Yang,[a, b] Xiao Chen,*[a] Qinggang Wang*[a]

a Key Laboratory of Biobased Materials, Qingdao Institute of Bioenergy and Bioprocess Technology, Chinese Academy of Sciences, Qingdao, 266101, China.

E-mail: chenxiao@qibebt.ac.cn, wangqg@qibebt.ac.cn

b Center of Materials Science and Optoelectronics Engineering, University of Chinese Academy of Sciences, Beijing, 100049, China.

‡These authors contribuated equally.

Table of Contents

1. General Information

All manipulations of air and/or moisture sensitive compounds were performed using standard Schlenk technique. Toluene, dichloromethane (DCM) and hexane were purchased from Sinopharm Chemical Reagent, dried over sodium benzophenone ketyl (toluene) or calcium hydride (DCM, hexane) and distilled under an argon atmosphere prior to use. ^{1}H and ^{13}C NMR spectra were recorded on a Bruker Avance III 400 MHz spectrometer using $CDCl_3$ as solvent and trimethylsilane (TMS) as internal reference. Chemical shifts and coupling constant were given in ppm and in Hz respectively. Attenuated total reflection-infrared (ATR-IR) spectroscopy was performed using Thermo Scientific Nicolet iN10. Elemental analysis was carried out on Vario EL III elemental analyzer at Shanghai Institute of Organic Chemistry, Chinese Academy of Sciences. Mass spectra for new organic compounds were measured using maXis II of Bruker Daltonics Corportion, while for Fe(II) complexes were recorded by ACQUITYTM UPLC & Q-TOF MS Premier at Analytical Center of Shanghai Jiao Tong University. X-ray Diffraction data was collected on Smart 1000 diffractometer with Mo K-alpha X-ray source (λ = 0.71073 Å) or Xcalibur/Gemini with Cu-Kα radiation (λ = 1.54178 Å). Molecular weights and polydispersity index (PDI) of polyisoprene were undertaken by gel permeation chromatography (GPC, Viscotek VE2001 GPC , Viscotek Corportion, USA) at 35 °C using a PL2MB500A column in THF at a flow rate of 1 $cm^3 \cdot min^{-1}$; 50 μL was injected using a Viscotek VE2001 GPC equipped with a Viscotek VE3580 Refractive Index detector using THF as the eluent. While high temperature gel permeation chromatography (HGPC, PL-GPC 220, Agilent Technologies, USA) was employed for polymerization using trichlorobenzene as the eluent and polystyrenes as standards. Isoprene was purchased from Aladdin Industrial Corporation, dried over CaH_2 and distilled prior to use. All other reagents were purchased from commercial sources and used without further purification. SCR-5 and SCR-10 natural rubbers were purchased from Qingdao Custom of China. A tensile testing machine (Shenzhen SANS, Guangdong province, China) was operated according to China standard, GB/T 528-92, at a tensile rate of 2 mm/min at room temperature. All tensile measurements were performed at least three times.

2. General Experimental Procedure

2.1 General Procedure For The Synthesis of Ligands

To a solution of 2-pyridinecarboxaldehyde (1.0 equiv) in CH_2Cl_2, amine (1.00 equiv) and activated 4 Å molecular sieves was added. The resulting mixture was stirred at room temperature for 12 hours. The reaction mixture was directly filtered through a celite plug and the solvent removed in vacuum to get the product.

2.2 General Procedure For The Synthesis of Complexs

In a glovebox, a solution of ligand (1.0 equiv) in CH_2Cl_2 was added to anhydrous $FeCl_2$ (1.0 equiv) in Schlenk flask. The mixture was stirred for 48 h at room temperature. Followed by filtration, concentration, washed by distilled hexane and dried under vacuum, the desired iron complexes were obtained as purple powders.

2.3 General Procedure For The Polymerization of Isoprene

Typical polymerization procedures: To a dried Schleck tube, iron(II) complexes, toluene, MAO cocatalyst and isoprene were added subsequently. The reaction was carried out under different conditions, and quenched with a diluted HCl solution of methanol (MeOH/HCl = 50/1). The polymer was collected, washed with methanol for three times, and dried under vacuum to constant weight.

3. Supplementary Data

Table S1 Isoprene polymerization under different interval time

Entry	Interval time	Act[a]	Yield [b]	Microstructure [c]			M_n[d] (10^5)	PDI[d]
				*cis*1,4	*trans*1,4	3,4		
1	6	1.02	>99	54	3	43	3.0	1.8
2	12	1.02	>99	55		45	2.7	1.7
3	24	0.53	51	55		45	2.3	1.8

General conditons: typical polymerization of isoprene were carried out with the 4.0 μmol iron complex in the presence of 500 equiv. MAO in 5 mL toluene under Ar for 10.0 min; addition sequence: Fe-solvent-MAO- interval time-isoprene; $[IP]_0$ = 4 M; Tol = 5 mL. [a] 10^6 g · (mol of Fe) $^{-1}$ · h $^{-1}$; [b] Isolated yield. [c] Determined by ^{1}H and ^{13}C NMR.[d] Determined by high temperature gel permeation chromatography (GPC) .

4. Analytical Data for Compounds

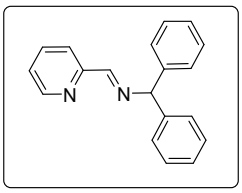

((E)-N-benzhydryl-1-(pyridin-2-yl) -methanimine) (2a): Prepared according to the general procedure (2.54 g, 88% yield). NMR Spectroscopy: **^{1}H NMR** (400 MHz, $CDCl_3$, 298 K) δ: 8.58 (d, *J* = 4.44 Hz, 1H), 8.52 (s, 1H), 8.18 (d, *J* = 7.92 Hz, 1H), 7.64 (t, *J* = 7.60 Hz, 1H), 7.39 (d, *J* = 7.40 Hz, 4H), 7.29 (t, *J* = 7.72 Hz, 4H), 7.20 (t, *J* = 7.20 Hz, 3H), 5.68 (s, 1H); **^{13}C NMR** (100 MHz, $CDCl_3$, 298 K), δ: 161.8, 154.5, 149.1, 143.1, 136.2, 128.3, 127.5, 127.0, 124.6, 121.3, 77.5. **HRMS-ESI** (m/z) $[M + Na]^+$ Calcd for $C_{19}H_{16}N_2$: 295.1206. Found, 295.1210.

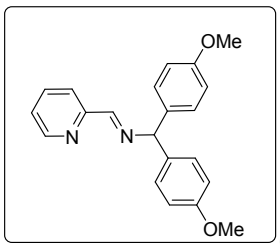

(E)-N-(bis(4-methoxyphenyl)methyl)-1-(pyridin-2-yl)methanimine (2b) Prepared according to the general procedure (0.6 g, 68% yield). **^{1}H NMR** (400 MHz, $CDCl_3$, 298 K) δ 8.63-8.62 (m, 1H), 8.47 (s, 1H), 8.20 (d, *J* = 7.92 Hz, 1H), 7.74 (dt, *J* = 1.40 Hz, *J* = 7.64 Hz, 1H), 7.32-7.25 (m, 5H), 6.87-6.84 (m, 4H), 5.63 (s, 1H), 3.78 (s, 6H); **^{13}C NMR** (100 MHz, $CDCl_3$, 298 K) δ161.4, 158.6, 154.8, 149.3, 136.4, 135.7, 128.7, 124.7, 121.4, 113.8, 55.2. **HRMS-ESI** (m/z) $[M + Na]^+$ Calcd for $C_{21}H_{20}N_2O_2$: 355.1422 . Found, 355.1421.

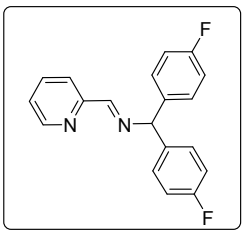

(E)-N-(bis(4-fluorophenyl)methyl)-1-(pyridin-2-yl)methanimine (2c). Prepared according to the general procedure (1.8 g, 90% yield). ^{1}H NMR (400 MHz, $CDCl_3$, 298 K) δ 8.65-8.63 (m, 1H), 8.49 (s, 1H), 8.19 (d, *J* = 7.92 Hz, 1H), 7.76 (dt, *J* = 1.24 Hz, *J* = 7.60 Hz, 1H), 7.34-7.30 (m, 5H), 7.04–6.99 (m, 4H), 5.65 (s, 1H); ^{13}C NMR (100 MHz, $CDCl_3$, 298 K) δ 163.1, 162.1, 160.7, 154.4, 149.4, 138.9, 138.8, 136.5, 129.2, 129.1, 125.0, 121.5, 115.4, 115.2, 76.0. **HRMS-ESI** (m/z) $[M + Na]^+$ Calcd for $C_{19}H_{14}F_2N_2$: 331.1023. Found, 331.1021.

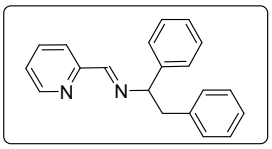

(E)-N-(1,2-diphenylethyl) -1-(pyridin-2-yl) methanimine (2d): Prepared according to the general procedure (2.52 g, 83% yield). NMR Spectroscopy: **^{1}H NMR** (400 MHz, $CDCl_3$, 298 K, δ): 8.55 (d, *J* = 4.44 Hz, 1H), 8.10 (s, 1H), 8.07 (d, *J* = 7.88 Hz, 1H), 7.68 (t, *J* = 7.16 Hz, 1H), 7.44 (d, *J* = 7.36 Hz, 2H), 7.32 (t, *J* = 7.32 Hz, 2H), 7.25-7.21 (m, 2H), 7.19-7.16 (m, 2H), 7.12(d, *J* = 7.0 Hz, 1H), 7.08 (d, *J* = 7.08 Hz, 2H), 4.57 (t, *J* = 6.80 Hz, 1H), 3.24 (d, *J* = 6.88 Hz, 2H); **^{13}C NMR** (100

MHz, $CDCl_3$, 298 K, δ): 161.0, 154.4, 149.2, 143.2, 138.4, 136.3, 129.6, 128.3, 128.0, 127.0, 126.1, 124.5, 121.3, 76.8, 45.3. **HRMS-ESI** (m/z) $[M + H]^+$ Calcd for $C_{20}H_{18}N_2$: 287.1548. Found, 287.1549.

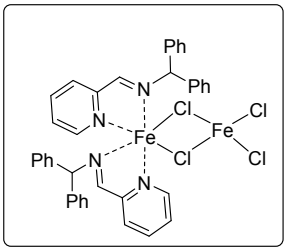

Iron complex 3a: Prepared according to the general procedure (140 mg, 70% yield). X-Ray quality crystals was grown from a saturation solution of the title compound in CH_2Cl_2 at -30 °C.**HRMS-ESI** (m/z) $[M\text{-}FeCl_3]^+$ Calcd for $C_{38}H_{32}Cl_4Fe_2N_4$: 635.1666. Found, 635.1660; **Elemental Analysis**: Calcd for $[C_{38}H_{32}Cl_4Fe_2N_4]$: C, 57.18; H, 4.04; N, 7.02; Found: C,57.71; H, 4.43; N, 6.71; **ATR-IR** (cm^{-1}): 1596, 1495, 1454, 1308, 1268, 1230, 1156, 1085, 1019, 1005, 991, 928, 864, 822, 796, 766, 741.

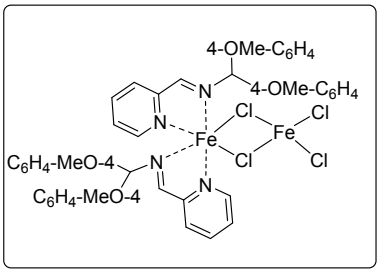

Iron complex 3b: Prepared according to the general procedure (389 mg, 85% yield). **HRMS-ESI** (m/z) $[M\text{-}FeCl_3]^+$ Calcd for $C_{42}H_{40}Cl_4Fe_2N_4O_4$: 755.2089; Found, 755.2078; **Elemental Analysis**: Calcd for $[C_{42}H_{40}Cl_4Fe_2N_4O_4]$: C, 54.93; H, 4.39; N, 6.10; Found: C, 54.59; H, 4.62; N, 6.01; **ATR-IR** (cm^{-1}): 1608, 1510, 1463, 1442, 1306, 1250, 1177, 1115, 1029, 907, 836, 818, 784, 767, 748.

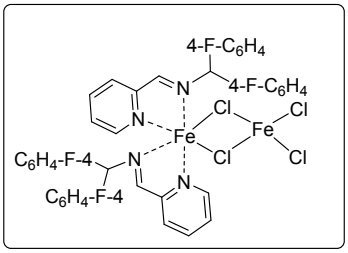

Iron complex 3c: Prepared according to the general procedure (247 mg, 80% yield). **HRMS-ESI** (m/z) $[M\text{-}FeCl_3]^+$ Calcd for $C_{38}H_{28}Cl_4F_4Fe_2N_4$: 707.1289; Found, 707.1295; **Elemental Analysis**: Calcd for$[C_{38}H_{28}Cl_4F_4Fe_2N_4]$: C, 52.45; H, 3.24; N, 6.44; Found: C, 52.89; H, 3.63; N,6.31; **ATR-IR** (cm^{-1}): 1598, 1507, 1443, 1414, 1308, 1227, 1159, 1103, 1052, 1018, 967, 910, 863, 839, 788, 767, 745.

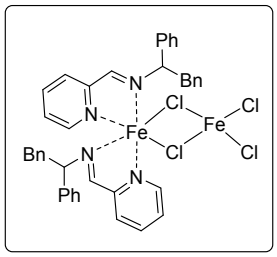

Iron complex 3d: Prepared according to the general procedure (175 mg, 85% yield). X-Ray quality crystals was grown from slowly evaporates from saturated solution of CH_2Cl_2 at room temperature **HRMS-ESI** (m/z) [M-$FeCl_3$]$^+$ Calcd for $C_{40}H_{36}Cl_4Fe_2N_4$, 663.1979; Found, 663.1981; **Elemental Analysis**: Calcd for[$C_{40}H_{36}Cl_4Fe_2N_4$]: C, 58.15; H, 4.39; N, 6.78; Found: C, 58.40; H,4.42; N, 6.52; ATR-IR (cm^{-1}): 1596, 1495, 1478, 1454, 1385, 1306, 1263, 1229, 1156, 1105, 1076, 1051, 1019, 901, 820, 760.

5. NMR Spectra of ligand and the Representative Polyisoprene

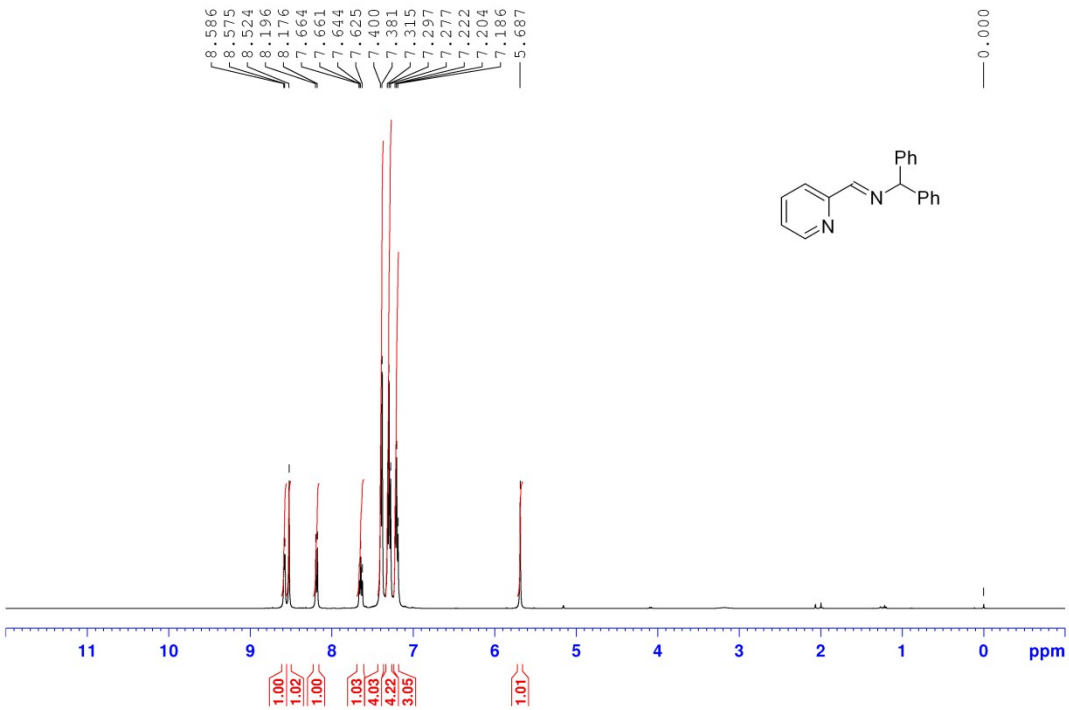

Figure S1. ^{1}H NMR spectrum (400 MHz, $CDCl_3$, 298 K) of **2a**

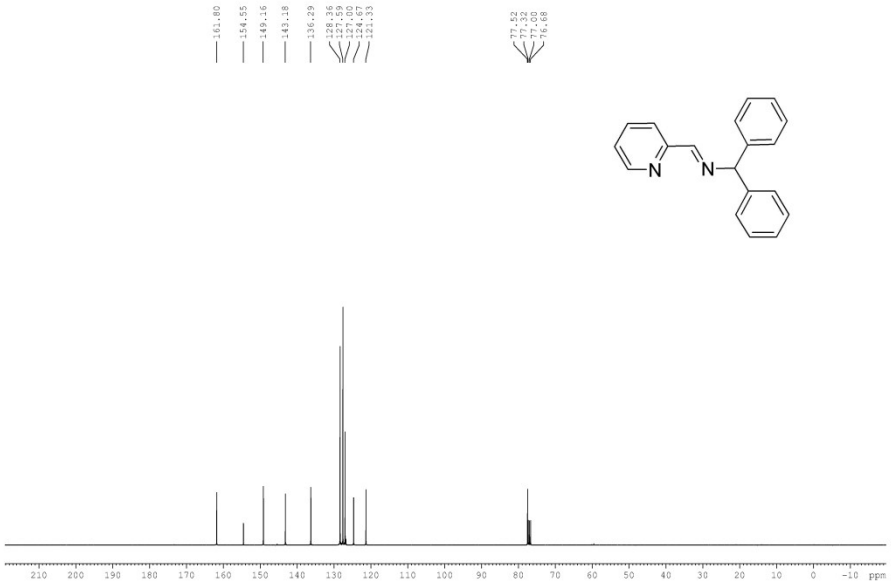

Figure S2. $^{13}C\{^{1}H\}$ NMR spectrum (100 MHz, $CDCl_3$, 298 K) of **2a**

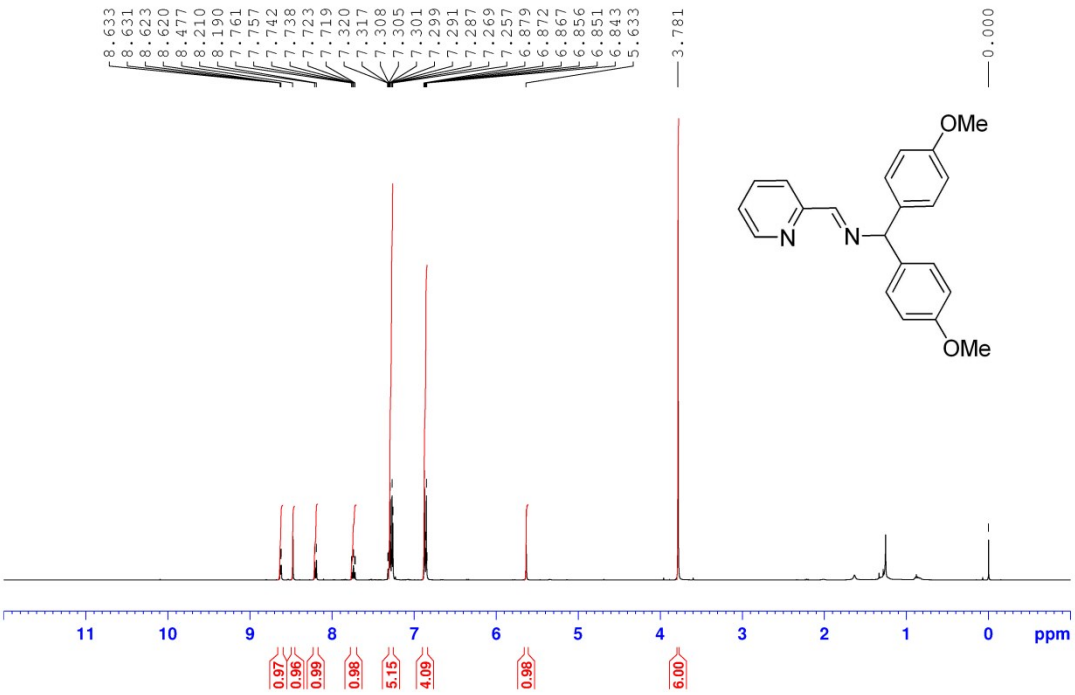

Figure S3. ^{1}H NMR spectrum (400 MHz, $CDCl_3$, 298 K) of **2b**

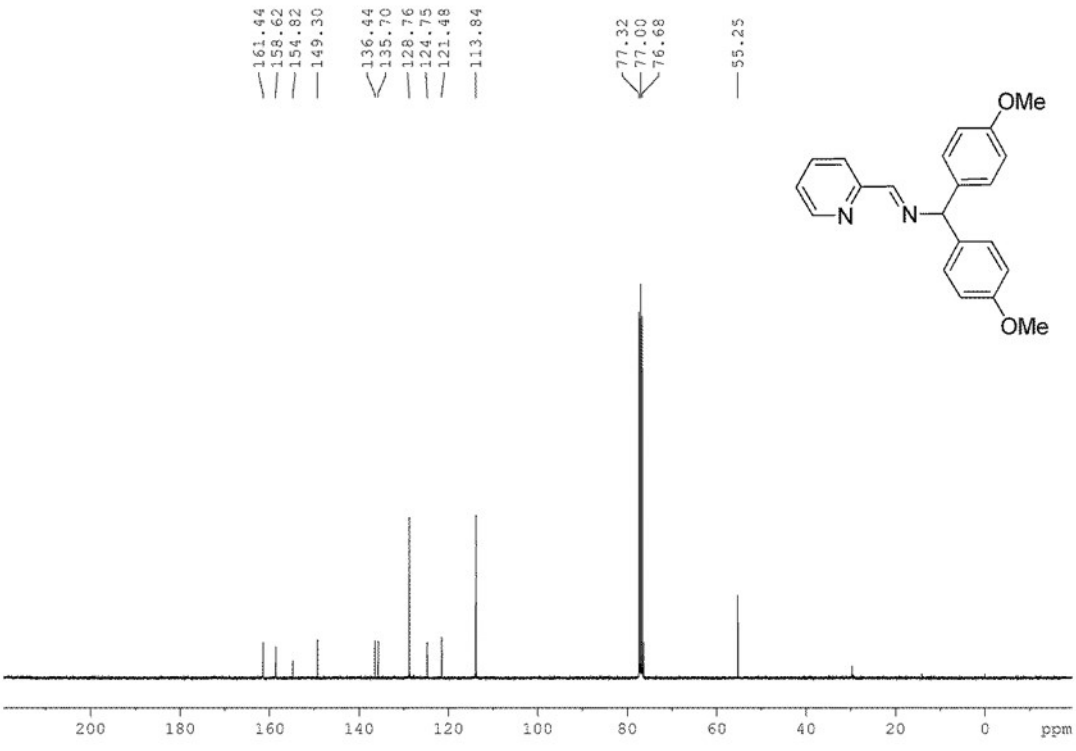

Figure S4. $^{13}C\{^{1}H\}$ NMR spectrum (100 MHz, $CDCl_3$, 298 K) of **2b**

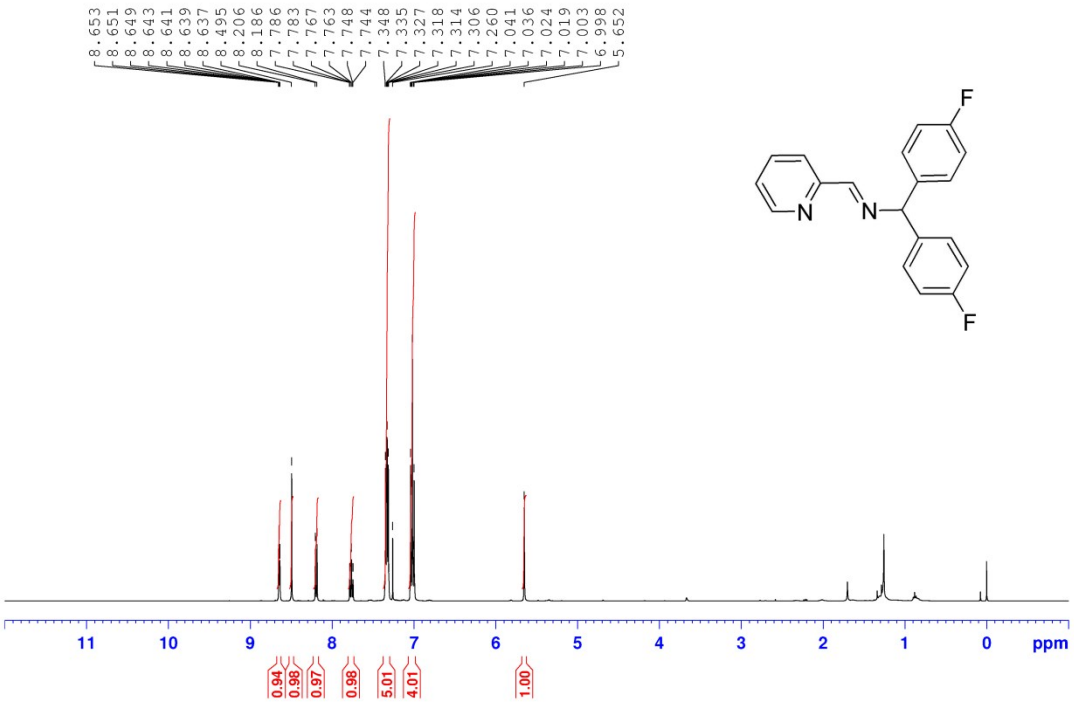

Figure S5. ^{1}H NMR spectrum (400 MHz, $CDCl_3$, 298 K) of **2c**

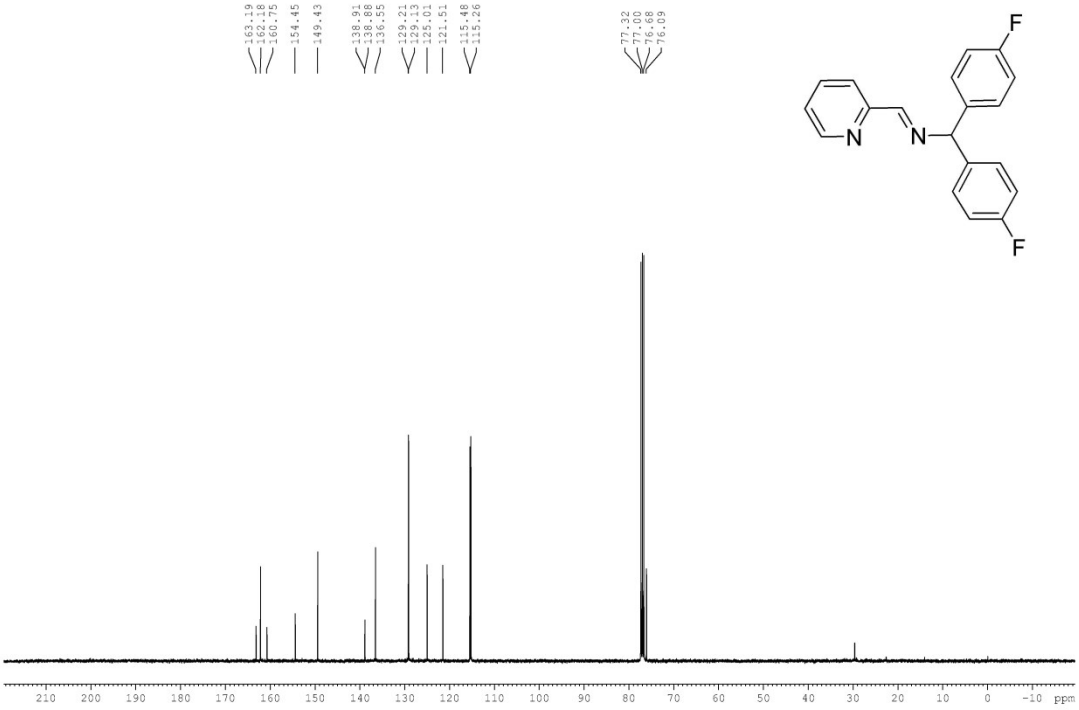

Figure S6. $^{13}C\{^{1}H\}$ NMR spectrum (400 MHz, $CDCl_3$, 298 K) of **2c**

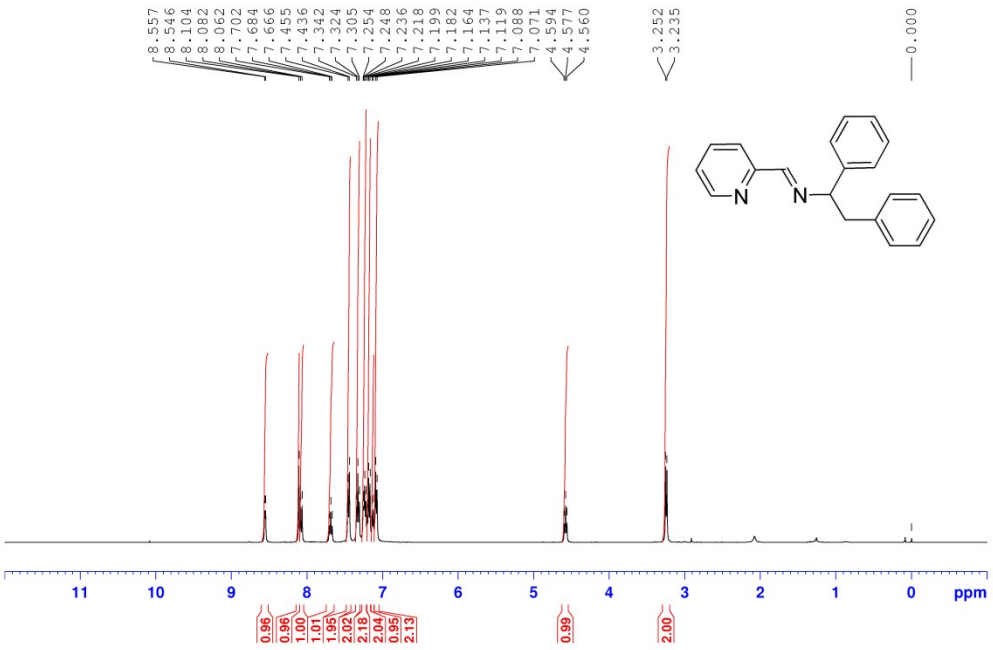

Figure S7. ^{1}H NMR spectrum (400 MHz, $CDCl_3$, 298 K) of **2d**

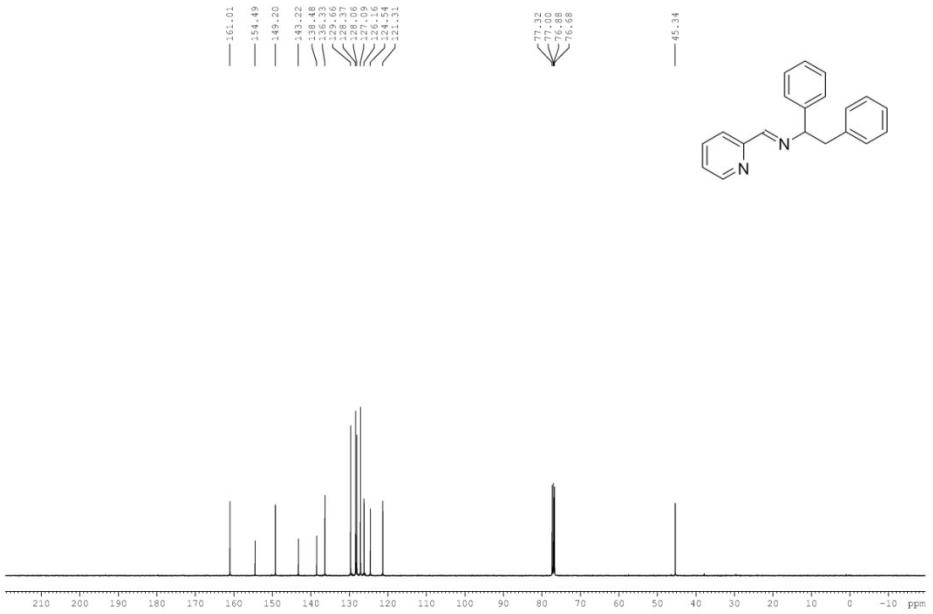

Figure S8. $^{13}C\{^{1}H\}$ NMR spectrum (100 MHz, $CDCl_3$, 298 K) of **2d**

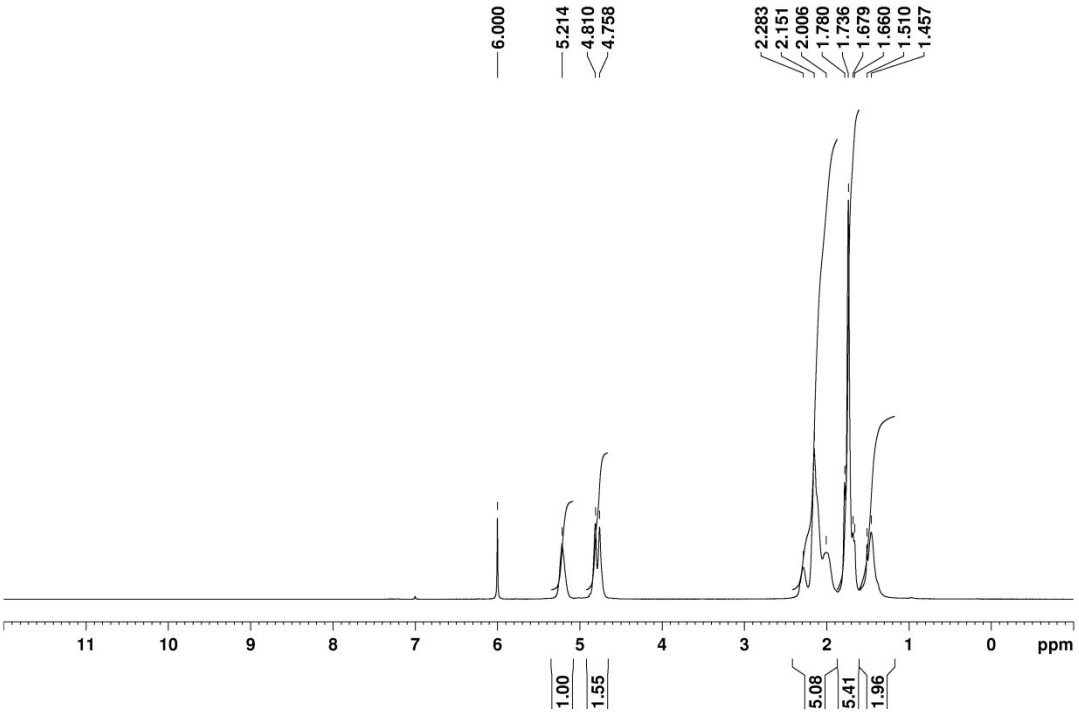

Figure S9. ^{1}H NMR spectrum (400 MHz, $C_2D_2Cl_4$, 393 K) of polyisoprene (Table 1, entry 1)

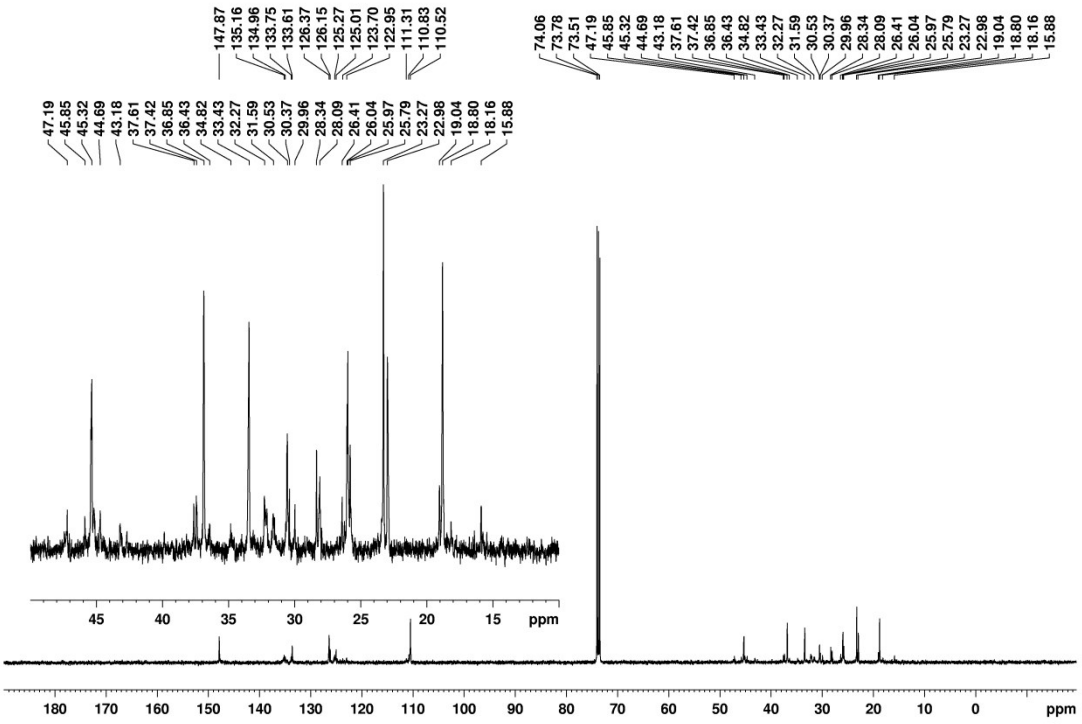

Figure S10. $^{13}C\{^{1}H\}$ NMR spectrum (100 MHz, $C_2D_2Cl_4$, 393 K) of polyisoprene (Table 1, entry 1)

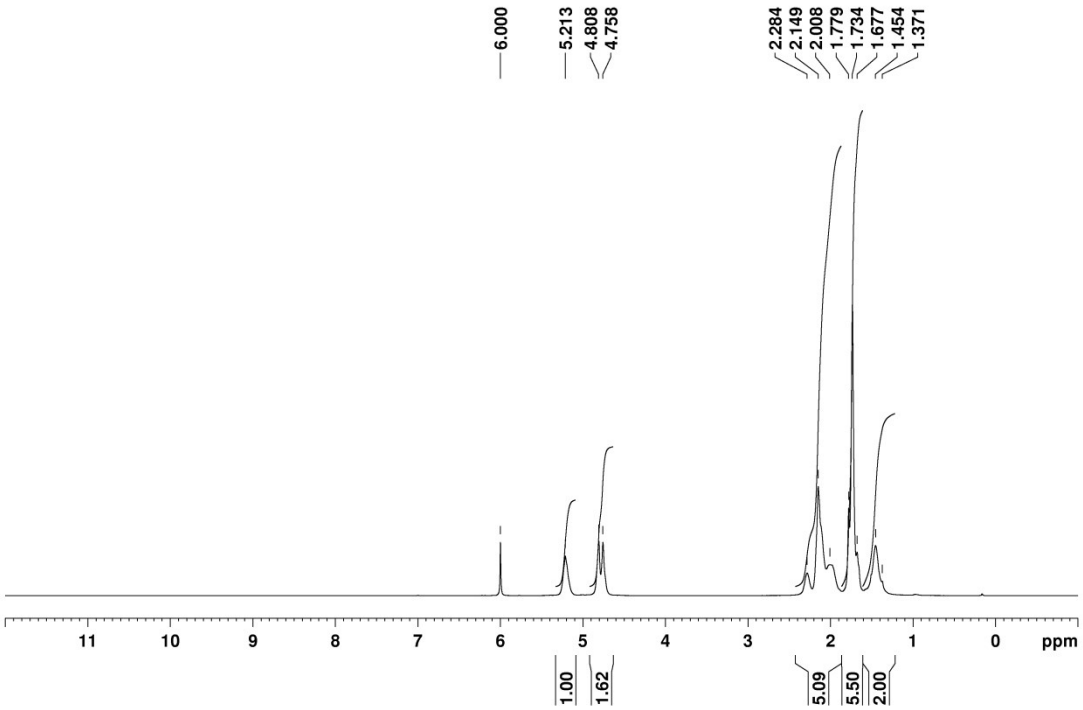

Figure S11. ^{1}H NMR spectrum (400 MHz, $C_2D_2Cl_4$, 393 K) of polyisoprene (Table 1, entry 2)

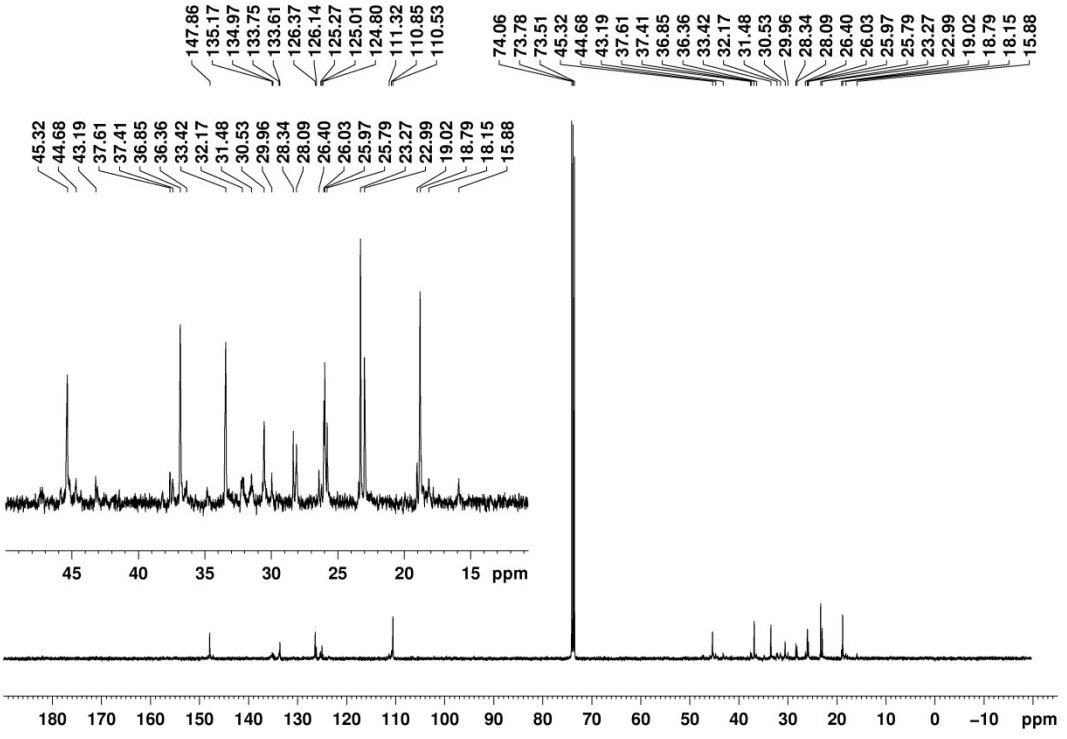

Figure S12. $^{13}C\{^{1}H\}$ NMR spectrum (100 MHz, $C_2D_2Cl_4$, 393 K) of polyisoprene (Table 1, entry 2)

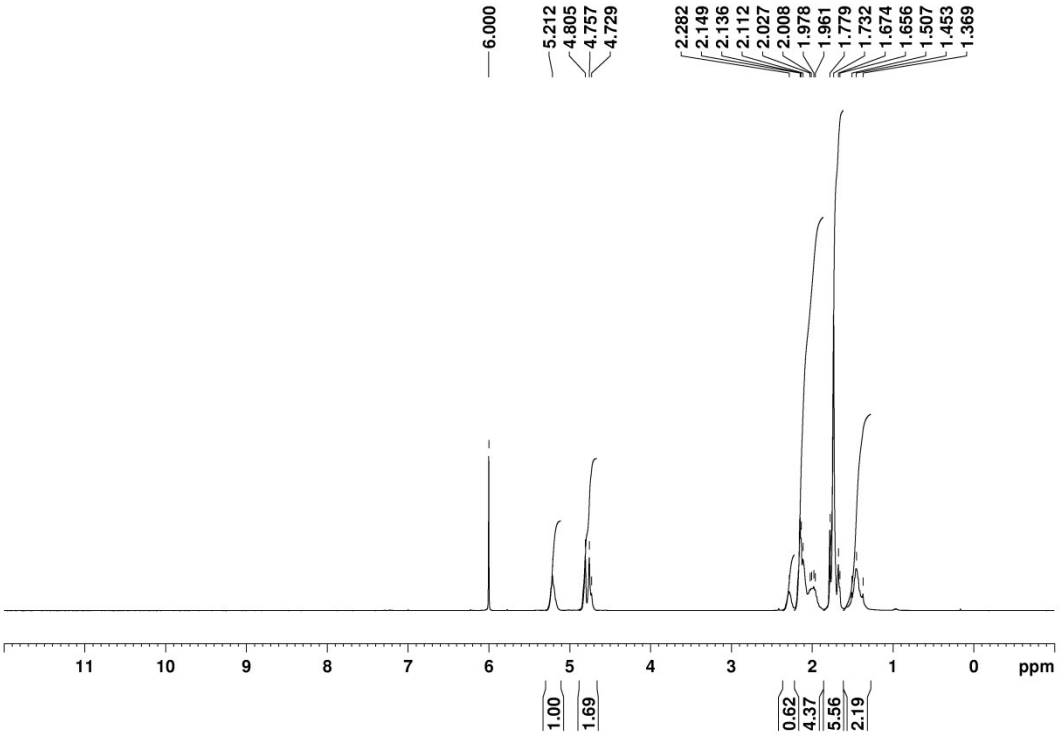

Figure S13. ^{1}H NMR spectrum (400 MHz, $C_2D_2Cl_4$, 393 K) of polyisoprene (Table 1, entry 4)

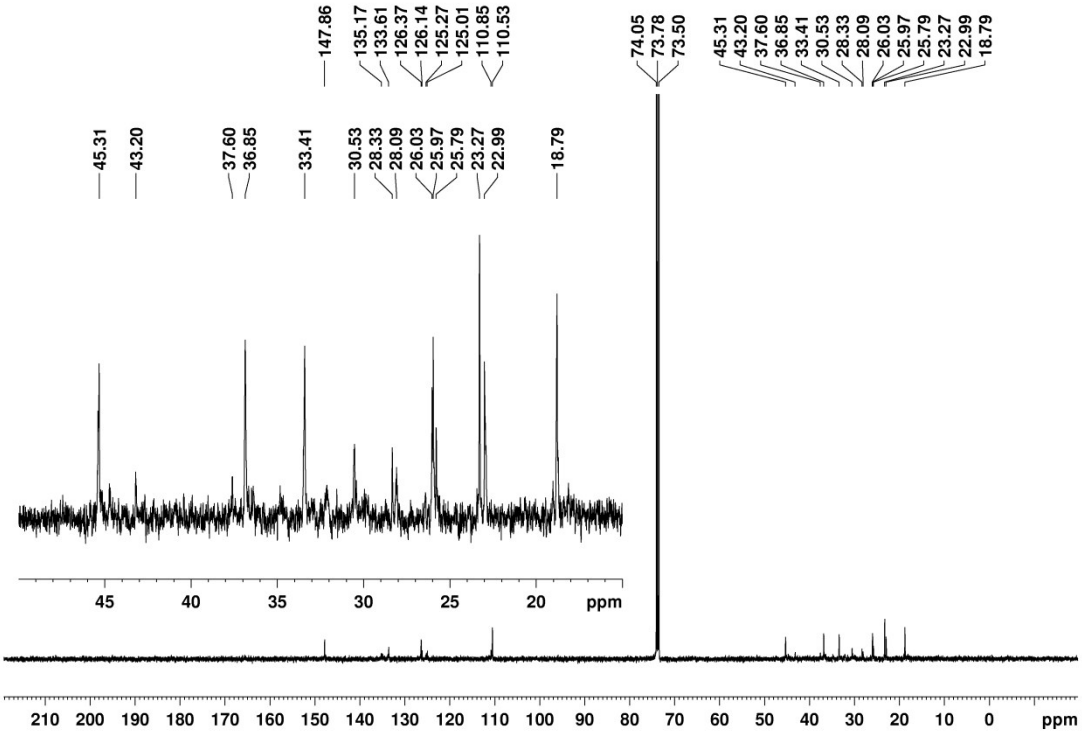

Figure S14. ^{13}C {^{1}H} NMR spectrum (100 MHz, $C_2D_2Cl_4$, 393 K) of polyisoprene (Table 1, entry 4)

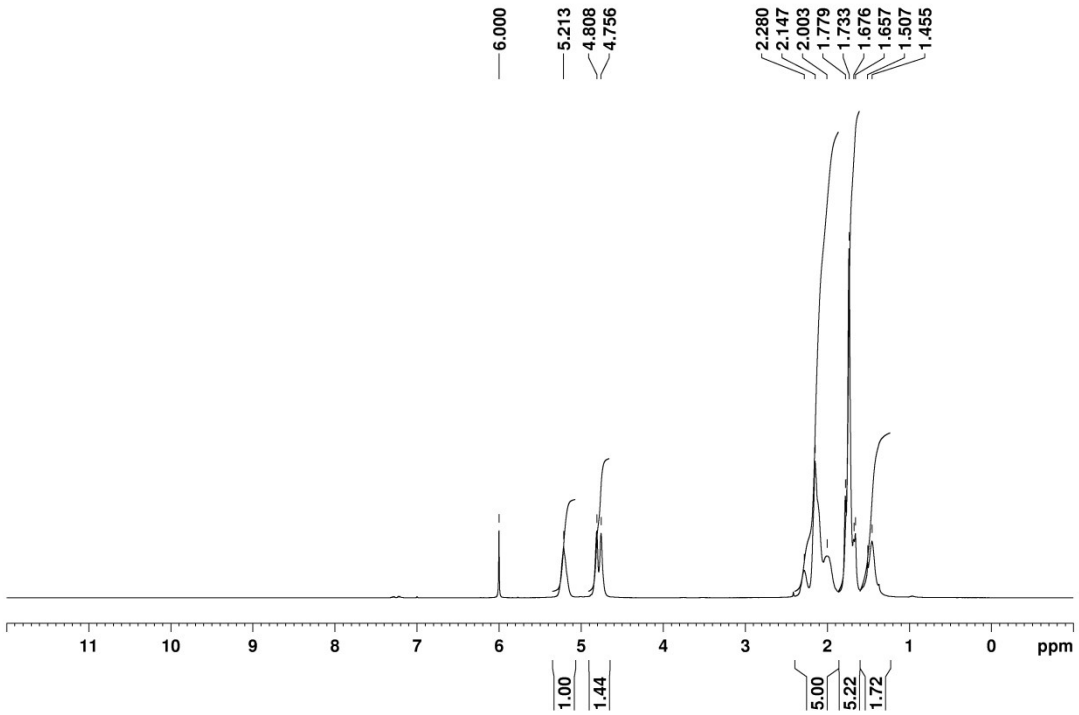

Figure S15. ^{1}H NMR spectrum (400 MHz, $C_2D_2Cl_4$, 393 K) of polyisoprene (Table 1, entry 5)

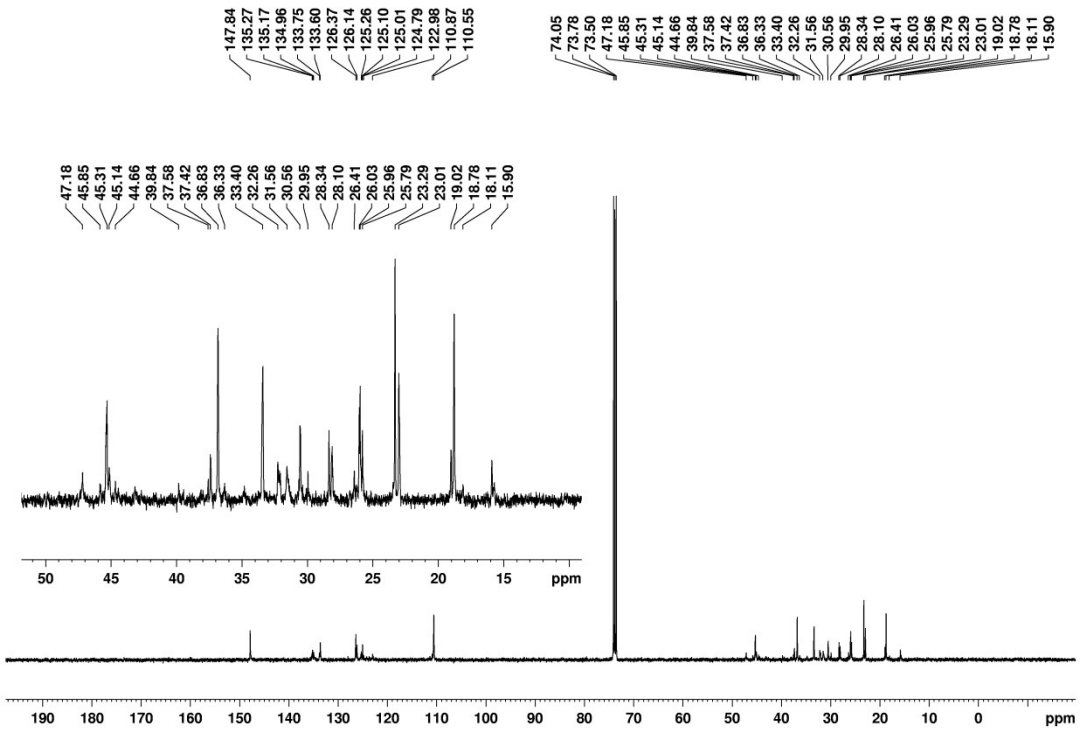

Figure S16. $^{13}C\{^{1}H\}$ NMR spectrum (100 MHz, $C_2D_2Cl_4$, 393 K) of polyisoprene (Table 1, entry 5)

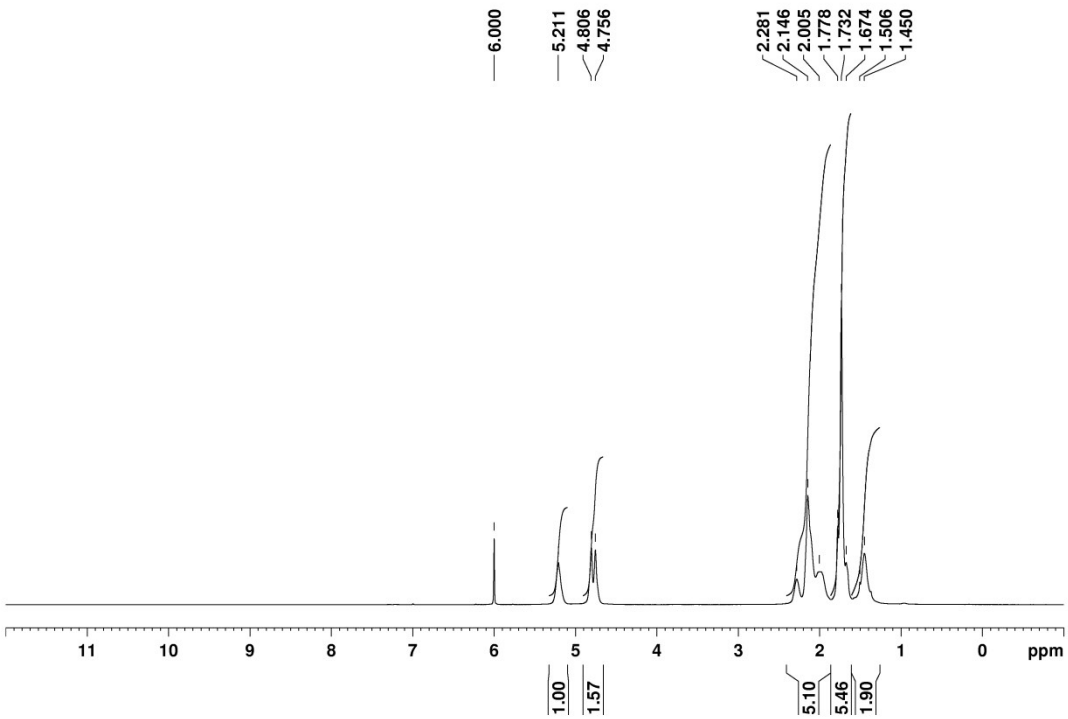

Figure S17. ^{1}H NMR spectrum (400 MHz, $C_2D_2Cl_4$, 393 K) of polyisoprene (Table 1, entry 6)

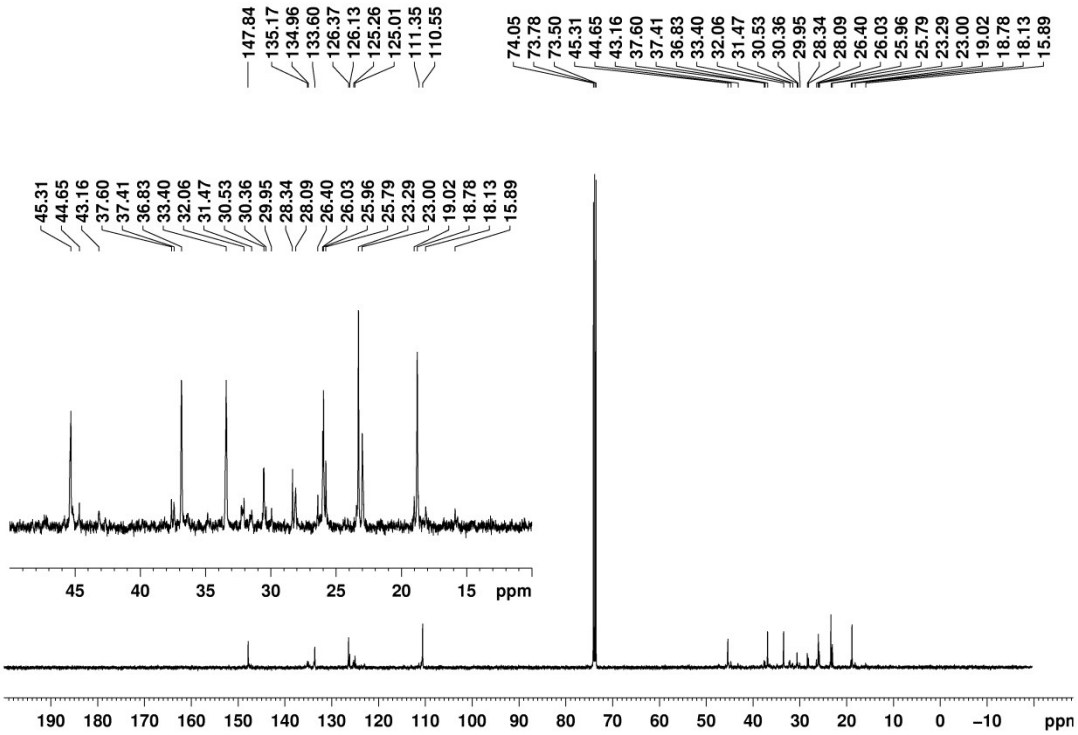

Figure S18. $^{13}C\{^{1}H\}$ NMR spectrum (100 MHz, $C_2D_2Cl_4$, 393 K) of polyisoprene (Table 1, entry 6)

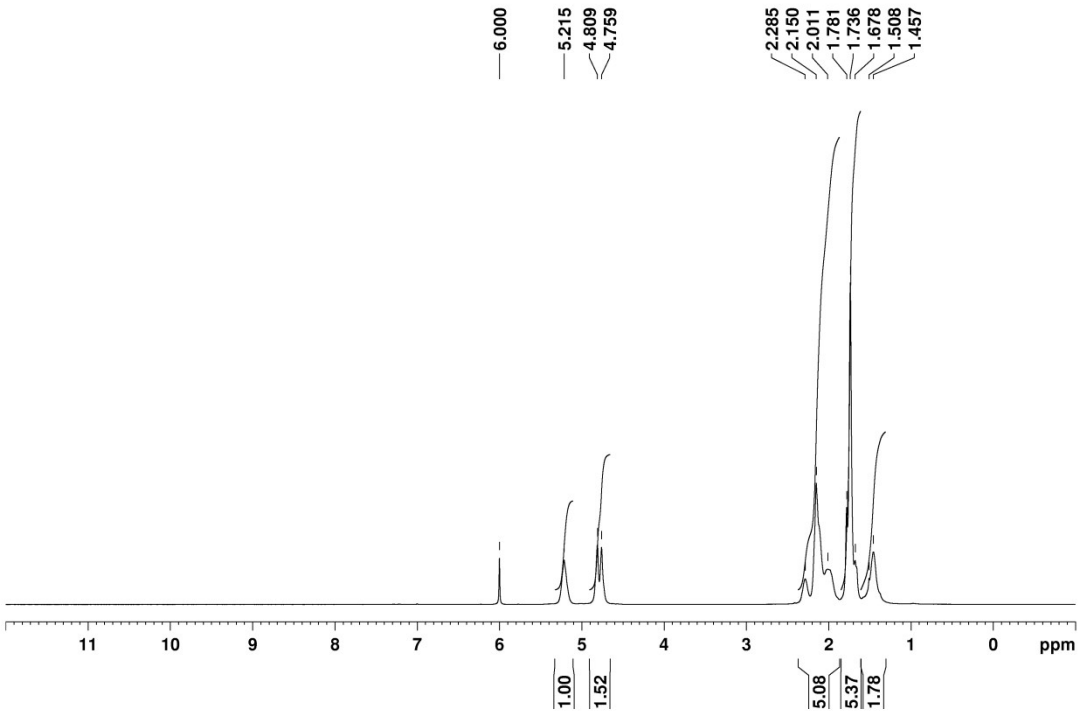

Figure S19. ^{1}H NMR spectrum (400 MHz, $C_2D_2Cl_4$, 393 K) of polyisoprene (Table 1, entry 7)

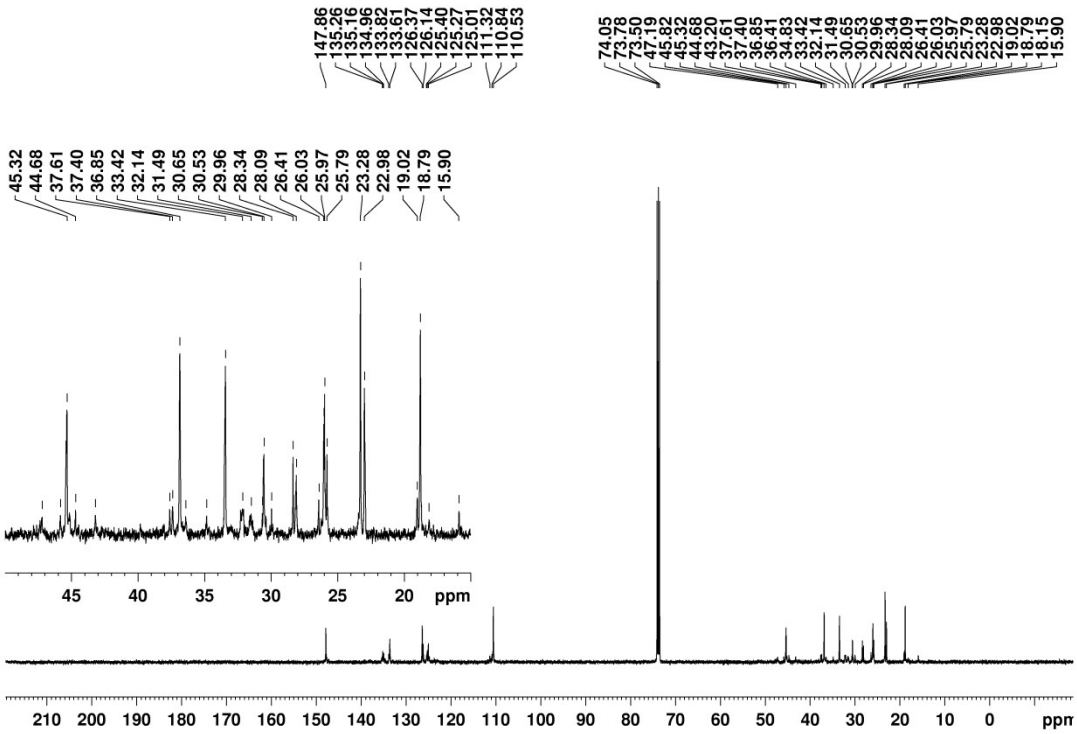

Figure S20. $^{13}C\{^{1}H\}$ NMR spectrum (100 MHz, $C_2D_2Cl_4$, 393 K) of polyisoprene (Table 1, entry7)

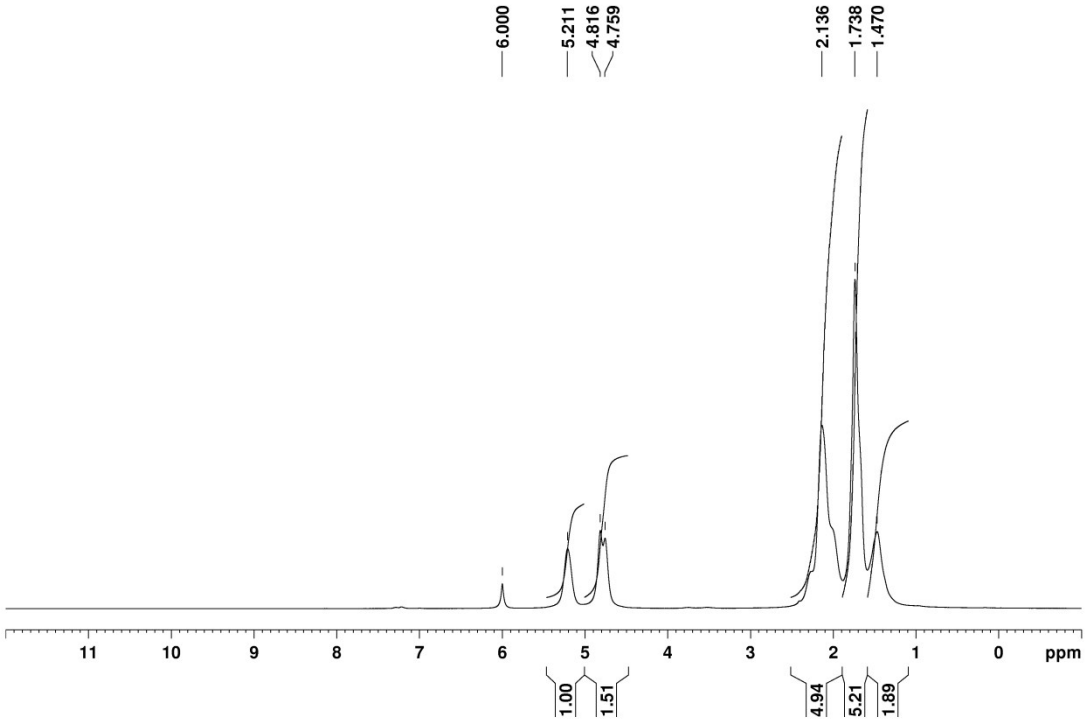

Figure S21. ^{1}H NMR spectrum (400 MHz, $C_2D_2Cl_4$, 393 K) of polyisoprene (Table 1, entry 8).

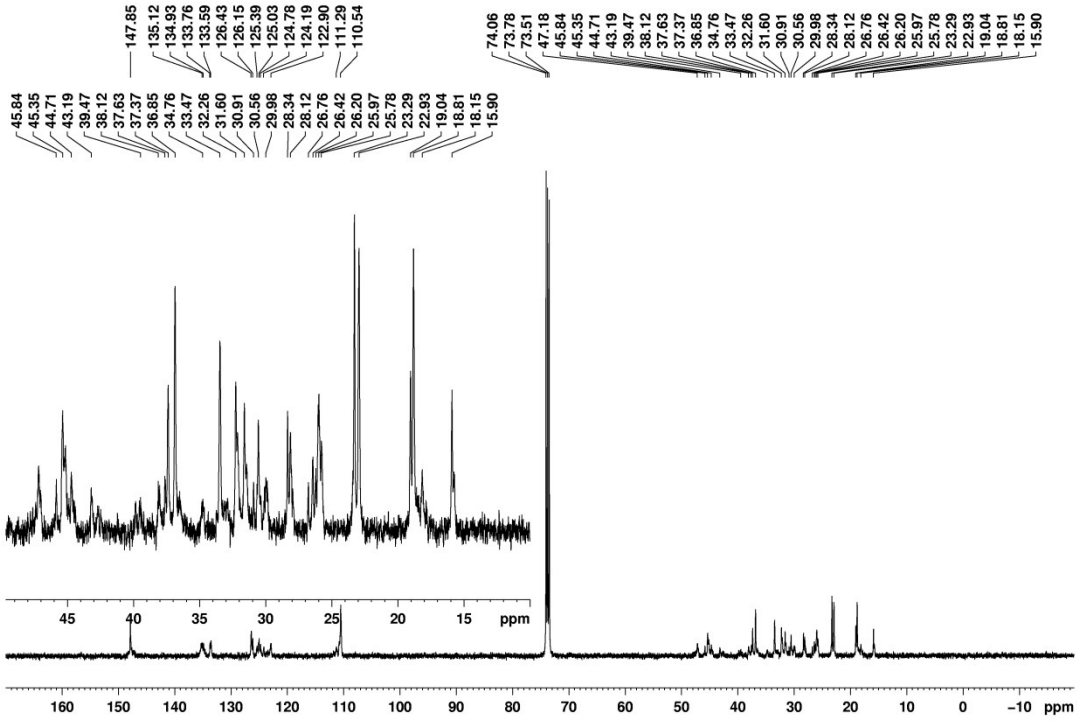

Figure S22. $^{13}C\{^{1}H\}$ NMR spectrum (100 MHz, $C_2D_2Cl_4$, 393 K) of polyisoprene (Table 1, entry 8)

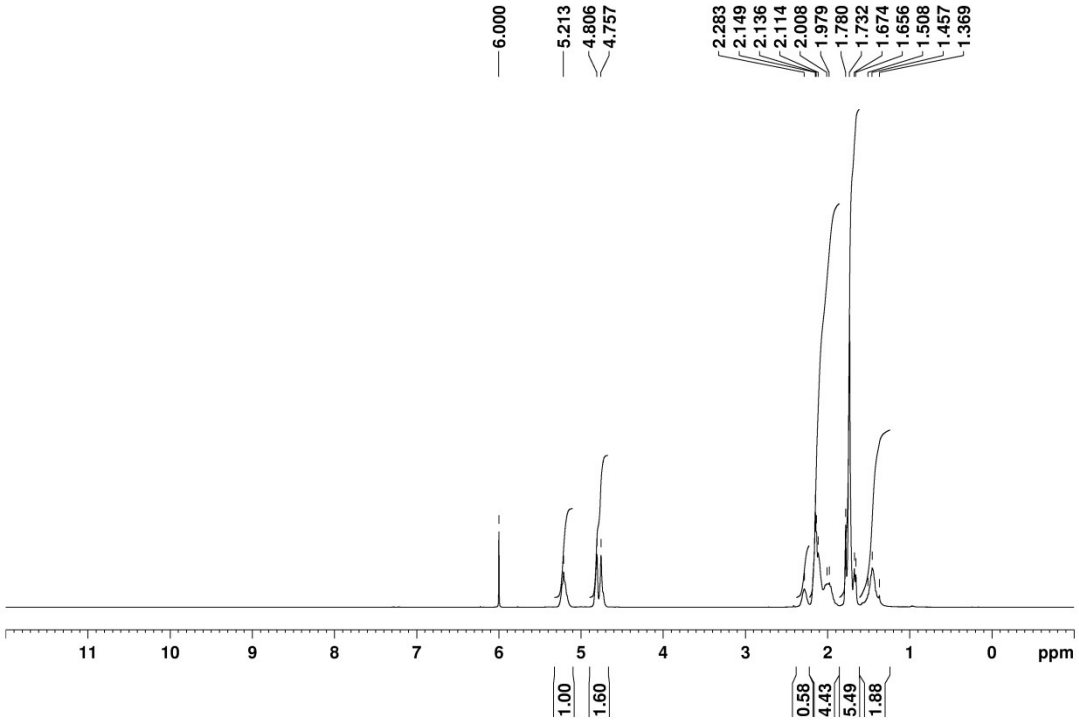

Figure S23. ^{1}H NMR spectrum (400 MHz, $C_2D_2Cl_4$, 393 K) of polyisoprene (Table 1, entry 9).

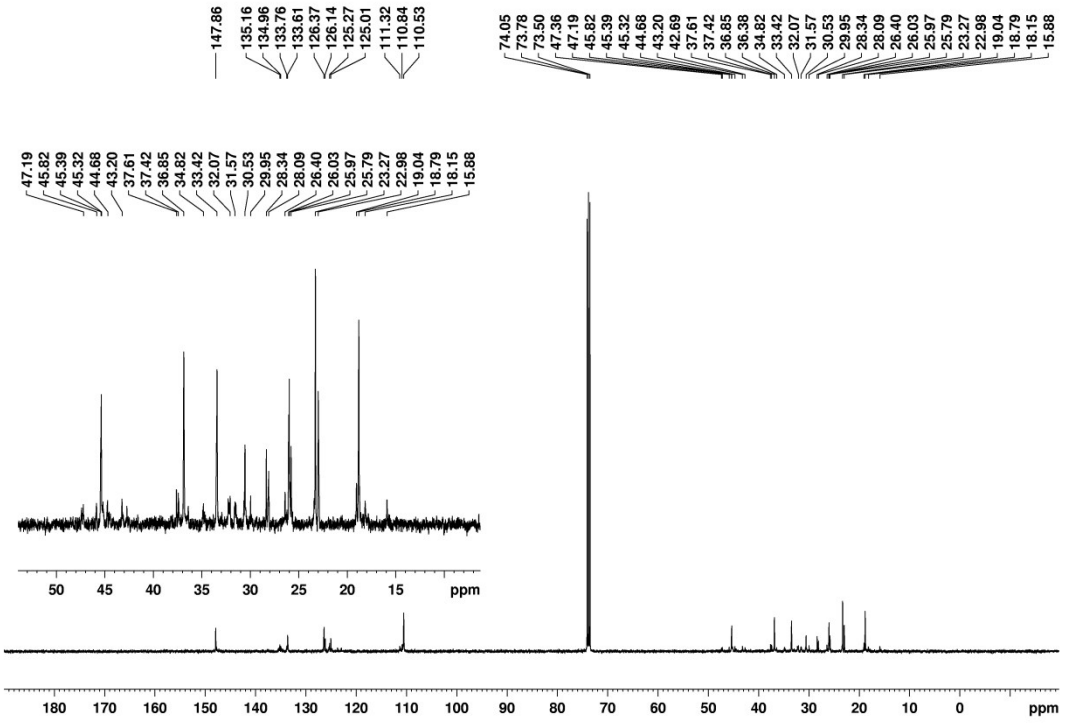

Figure S24. $^{13}C\{^{1}H\}$ NMR spectrum (100 MHz, $C_2D_2Cl_4$, 393 K) of polyisoprene (Table 1, entry 9)

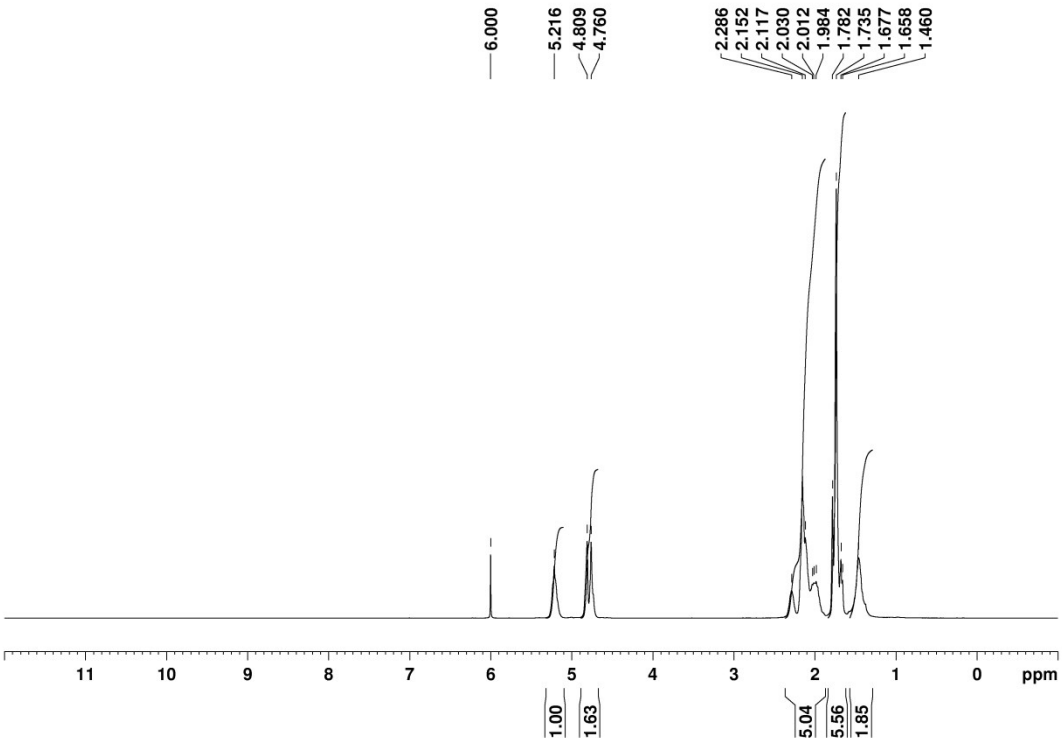

Figure S25. ^{1}H NMR spectrum (400 MHz, $C_2D_2Cl_4$, 393 K) of polyisoprene (Table 1, entry 10).

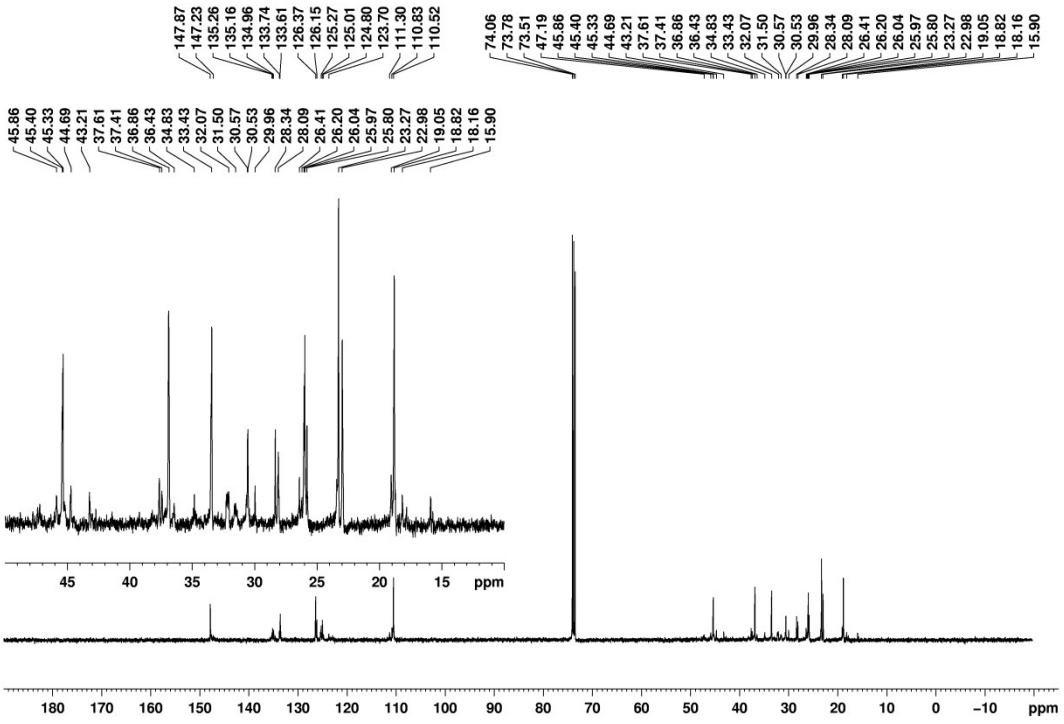

Figure S26. $^{13}C\{^{1}H\}$ NMR spectrum (100 MHz, $C_2D_2Cl_4$, 393 K) of polyisoprene (Table 1, entry 10)

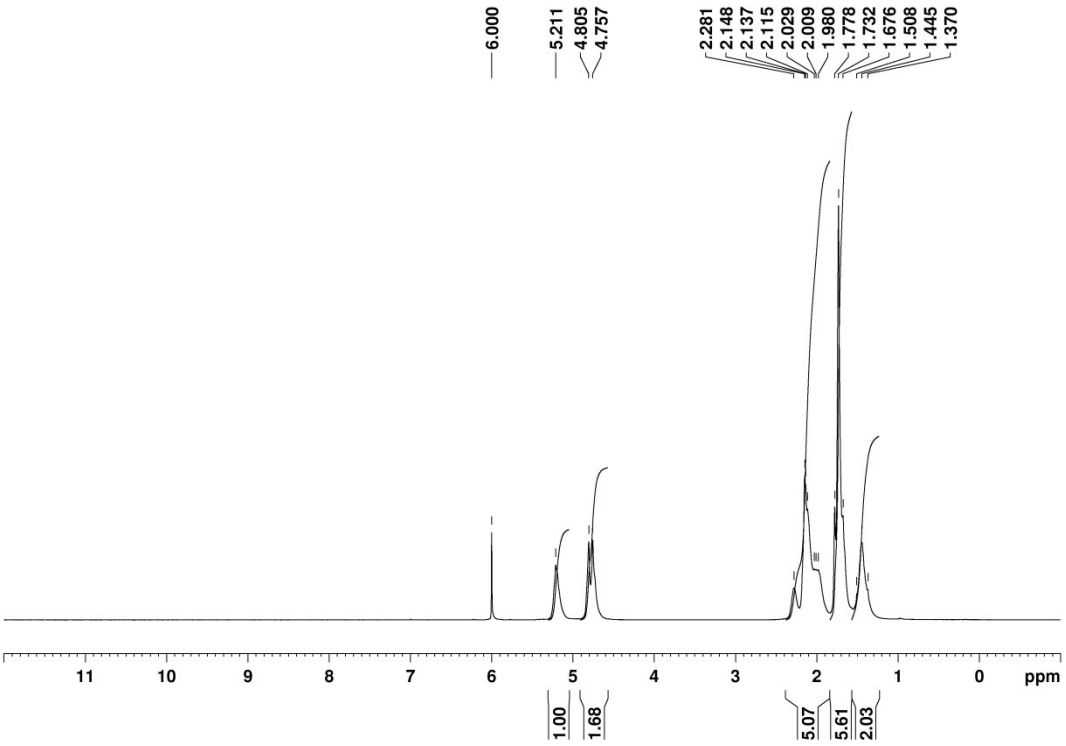

Figure S27. ^{1}H NMR spectrum (400 MHz, $CDCl_3$, 298 K) of polyisoprene (Table 1, entry 11).

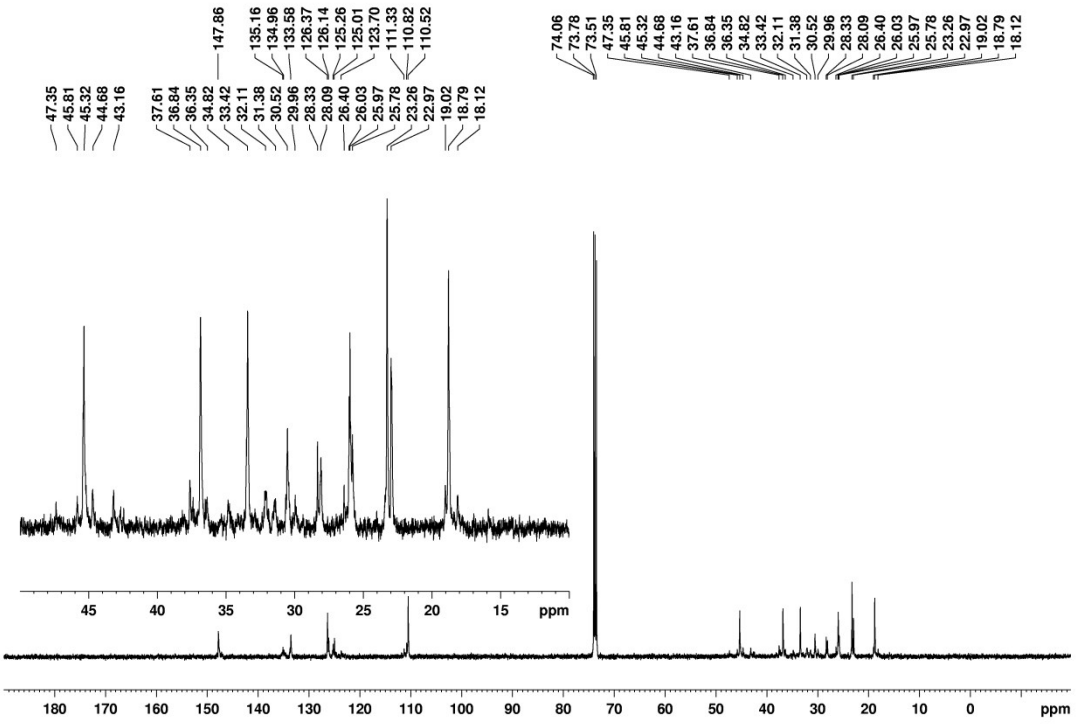

Figure S28. $^{13}C\{^{1}H\}$ NMR spectrum (100 MHz, $C_2D_2Cl_4$, 393 K) of polyisoprene (Table 1, entry 11)

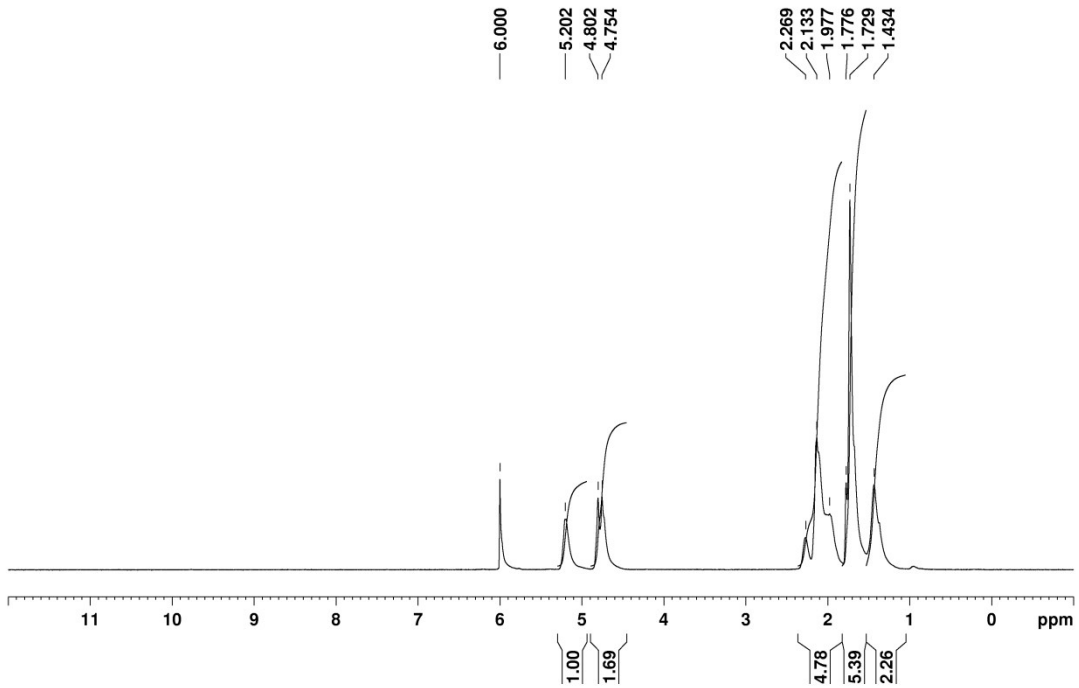

Figure S29. ^{1}H NMR spectrum (400 MHz, $C_2D_2Cl_4$, 393 K) of polyisoprene (Table 1, entry 12).

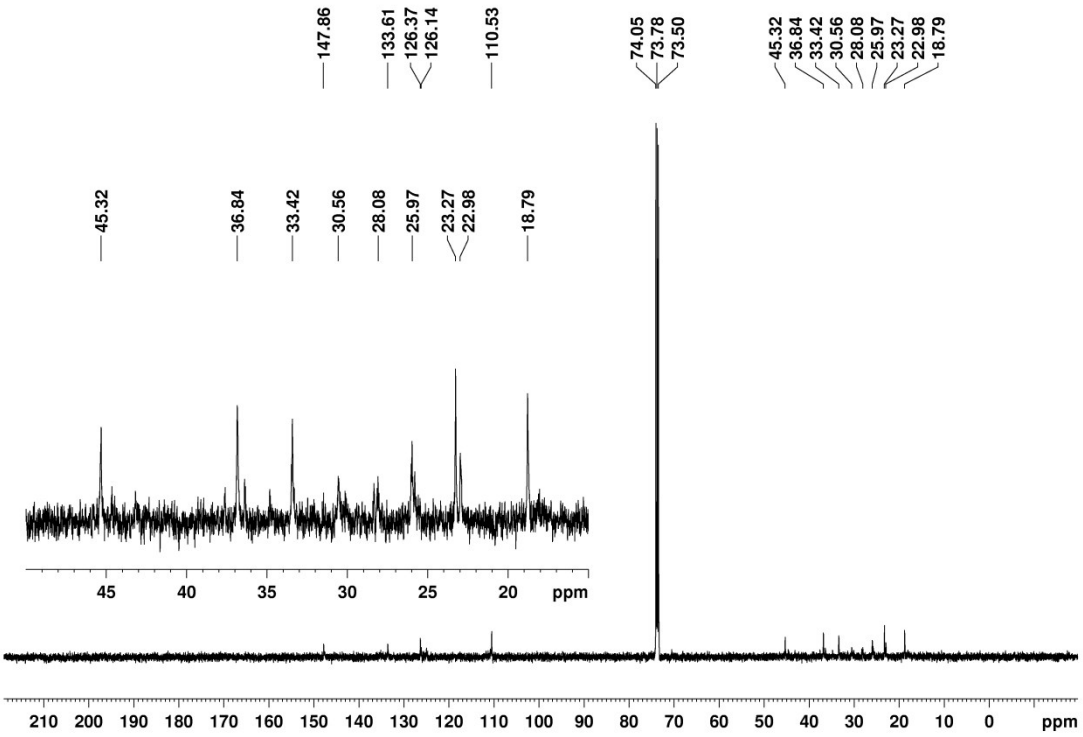

Figure S30. $^{13}C\{^{1}H\}$ NMR DEPT spectrum (100 MHz, $C_2D_2Cl_4$, 393 K) of polyisoprene (Table 1, entry 12)

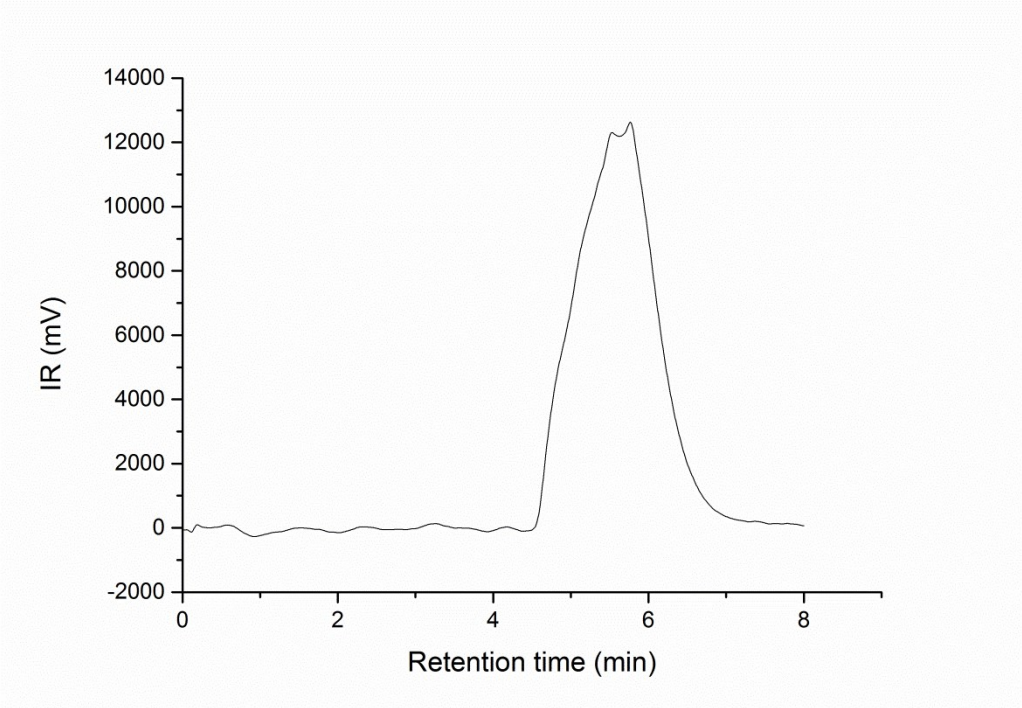

Molecular Weight Averages

Peak	Mp	Mn	Mw	Mz	Mz+1	Mv	PD
Peak 1	306524	267169	707905	1400316	2029072	1302644	2.65

Figure S31. The GPC of Fe(II) complex **3a** catalyzed polyisoprene (Table 1, entry 1).

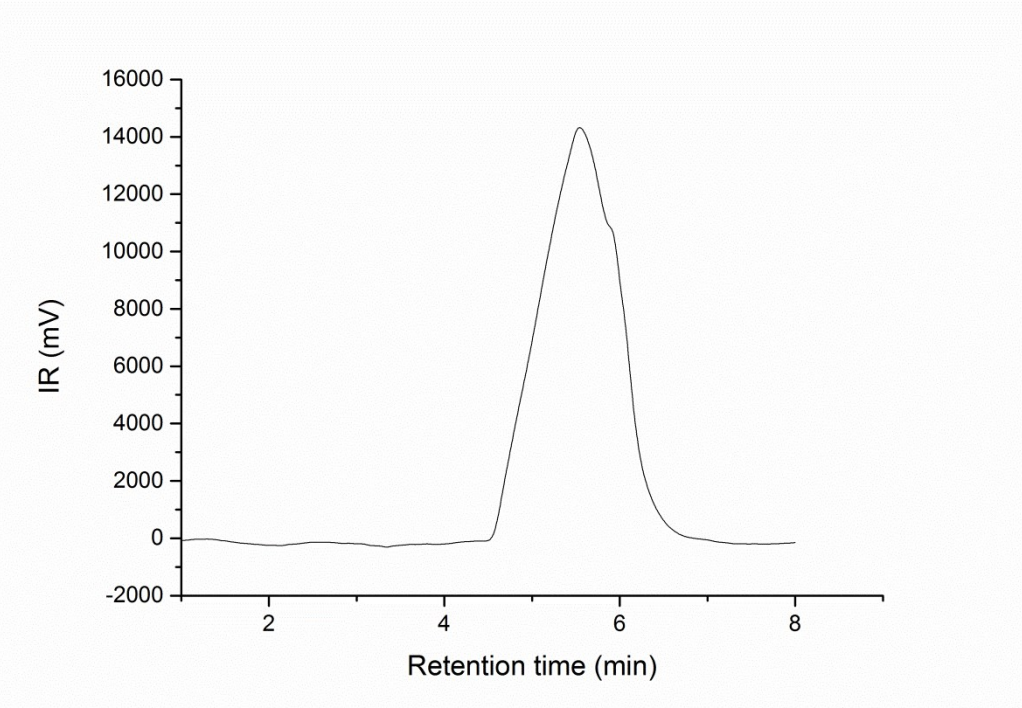

Molecular Weight Averages

Peak	Mp	Mn	Mw	Mz	Mz+1	Mv	PD
Peak 1	709345	474198	1079812	2069452	3100318	1918784	2.277

Figure S32. the GPC of Fe(II) complex **3a** catalyzed polyisoprene, Al : Fe = 20 (Table 1, entry 2).

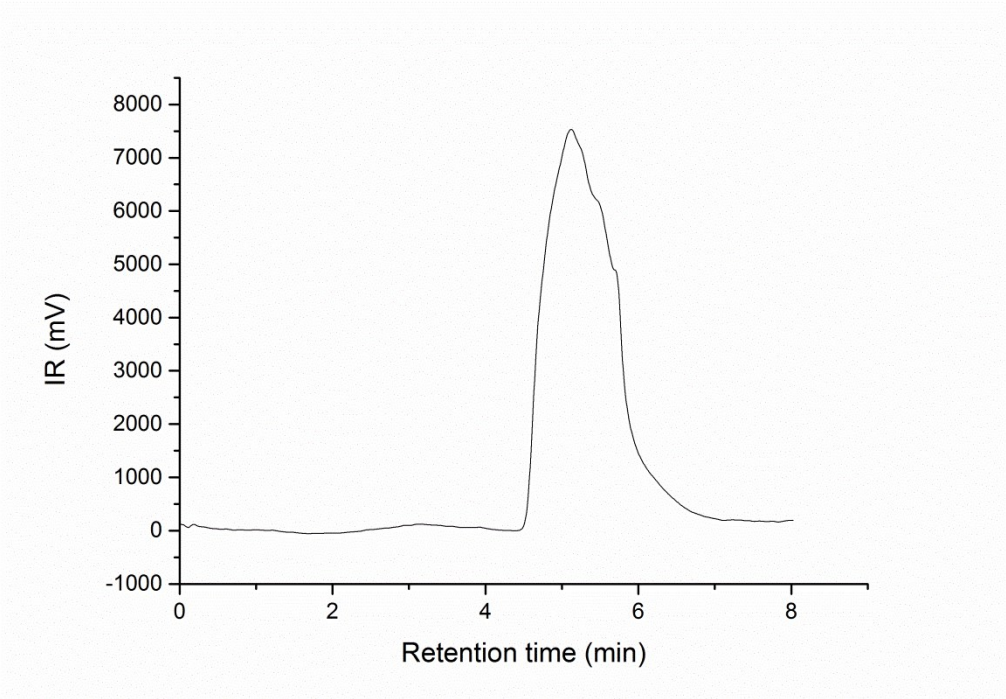

Molecular Weight Averages

Peak	Mp	Mn	Mw	Mz	Mz+1	Mv	PD
Peak 1	1829926	702332	1752408	2819803	3642758	2686092	2.495

Figure S33. the GPC of Fe(II) complex **3a** catalyzed polyisoprene, T = 0℃ (Table 1, entry 4).

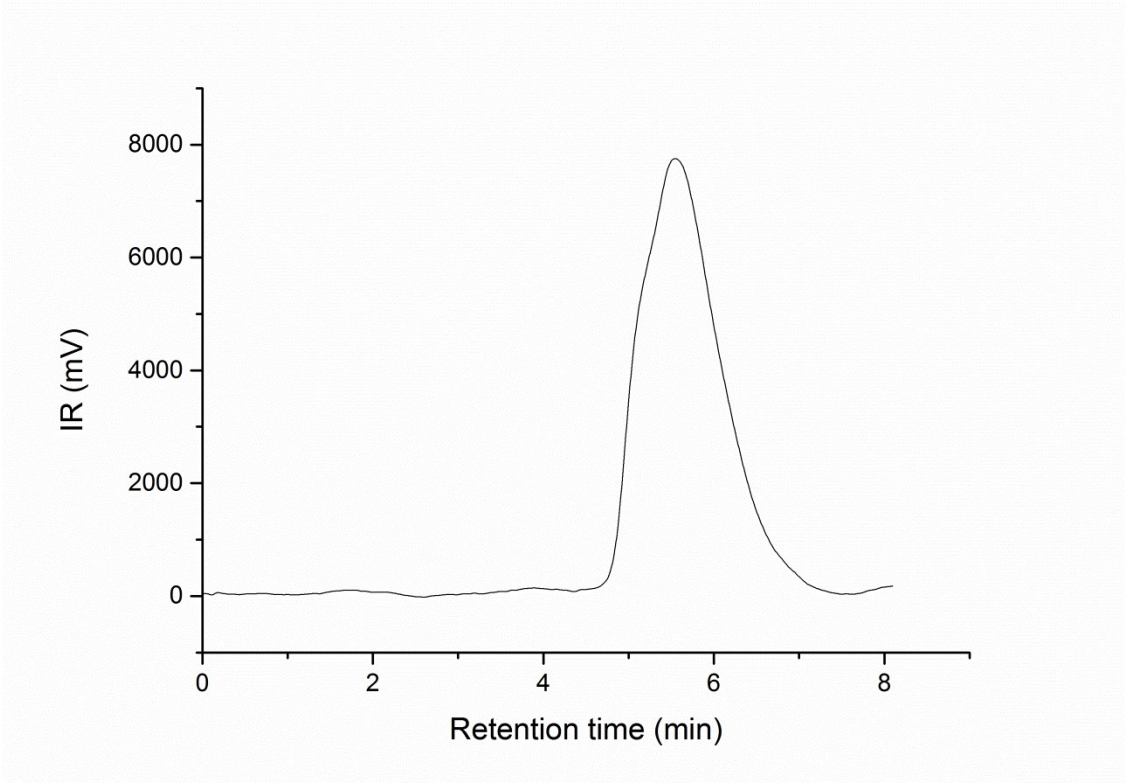

Molecular Weight Averages

Peak	Mp	Mn	Mw	Mz	Mz+1	Mv	PD
Peak 1	709345	301923	823407	1471710	2086909	1382376	2.727

Figure S34. the GPC of Fe(II) complex **3a** catalyzed polyisoprene, T = 50℃(Table 1, entry 5).

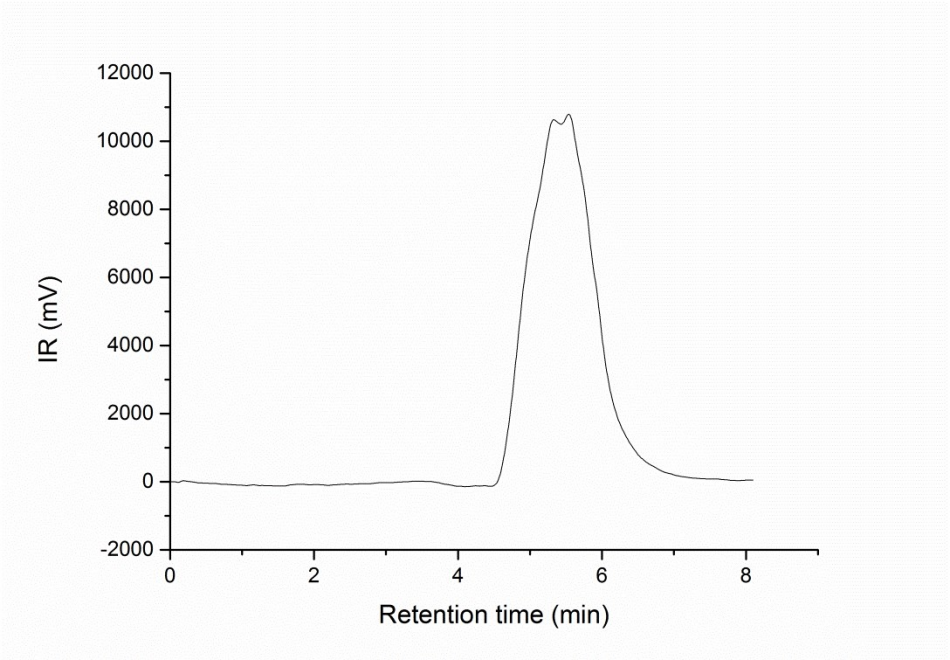

Molecular Weight Averages

Peak	Mp	Mn	Mw	Mz	Mz+1	Mv	PD
Peak 1	722649	484081	1200915	2082398	2896660	1959174	2.481

Figure S35. The GPC of Fe(II) complex **3b** catalyzed polyisoprene (Table 1, entry 6)

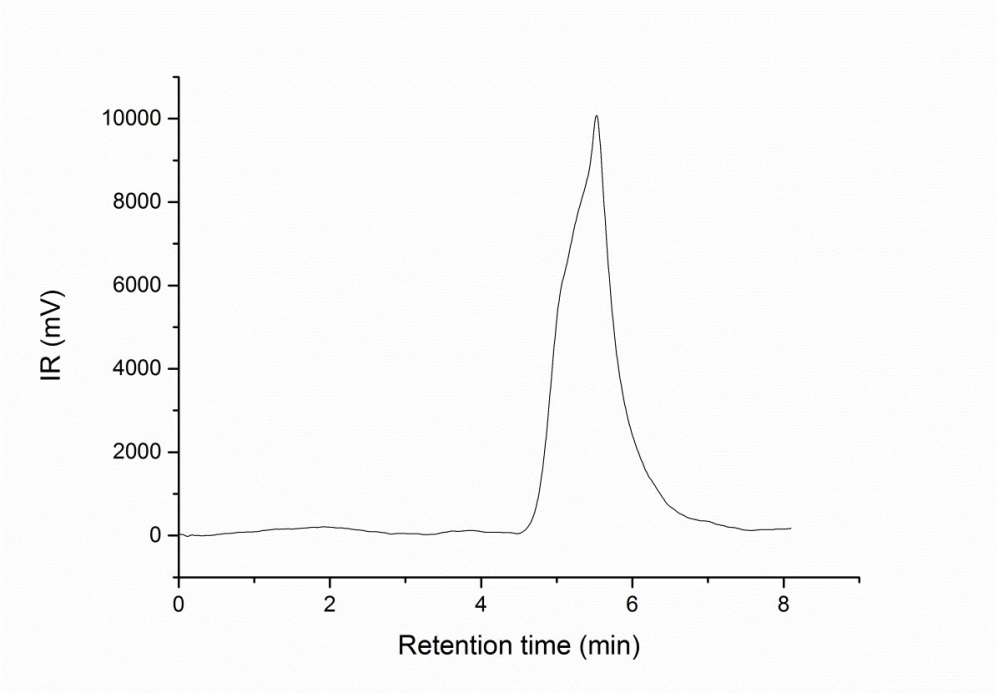

Molecular Weight Averages

Peak	Mp	Mn	Mw	Mz	Mz+1	Mv	PD
Peak 1	736203	504425	1123766	1774689	2394533	1683154	2.228

Figure S36. The GPC of Fe(II) complex **3c** catalyzed polyisoprene (Table 1, entry 7)

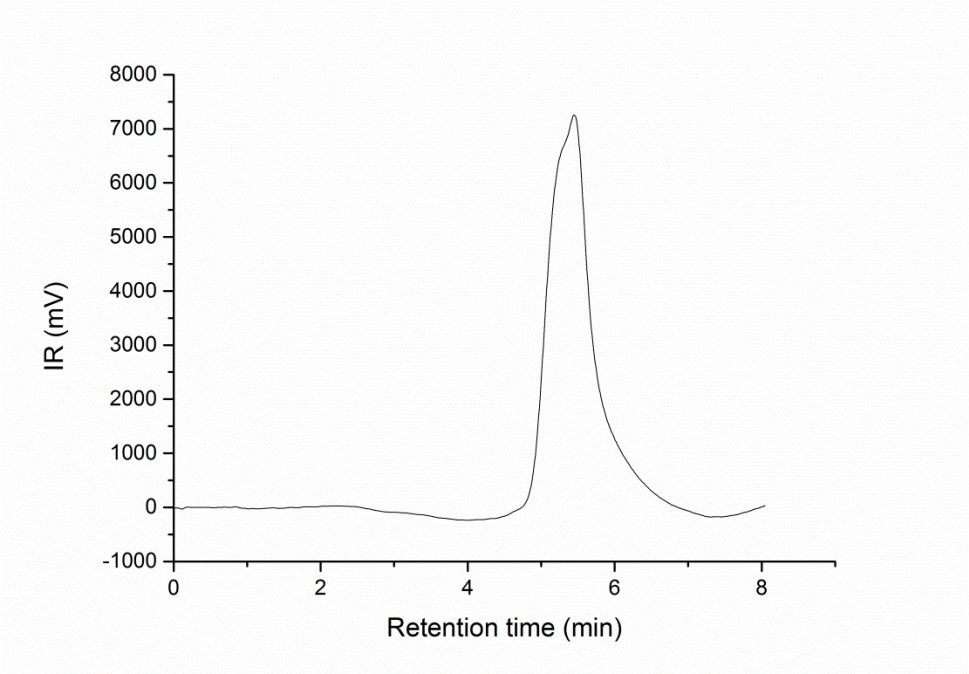

Molecular Weight Averages

Peak	Mp	Mn	Mw	Mz	Mz+1	Mv	PD
Peak 1	886541	466246	1072617	1662863	2521026	1567080	2.301

Figure S37. The GPC of Fe(II) complex **3d** catalyzed polyisoprene (Table 1, entry 8)

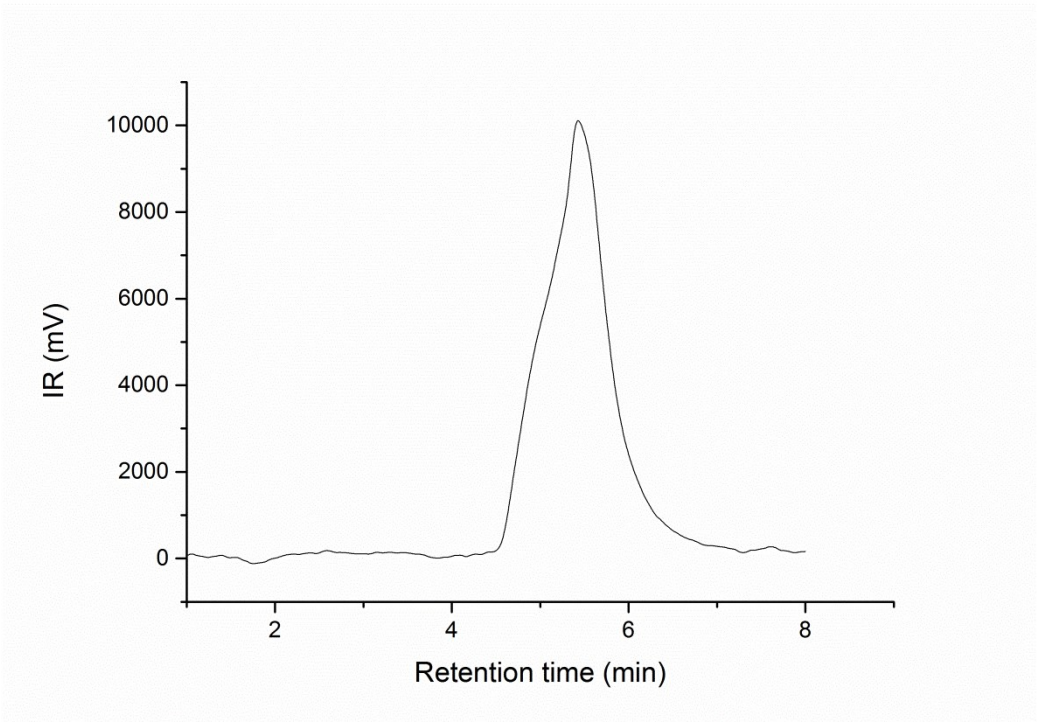

Molecular Weight Averages

Peak	Mp	Mn	Mw	Mz	Mz+1	Mv	PD
Peak 1	920108	528785	1294585	2240928	3184063	2101919	2.448

Figure S38. The GPC of polyisoprene at IP : Fe = 5000:1(Table 1, entry 9)

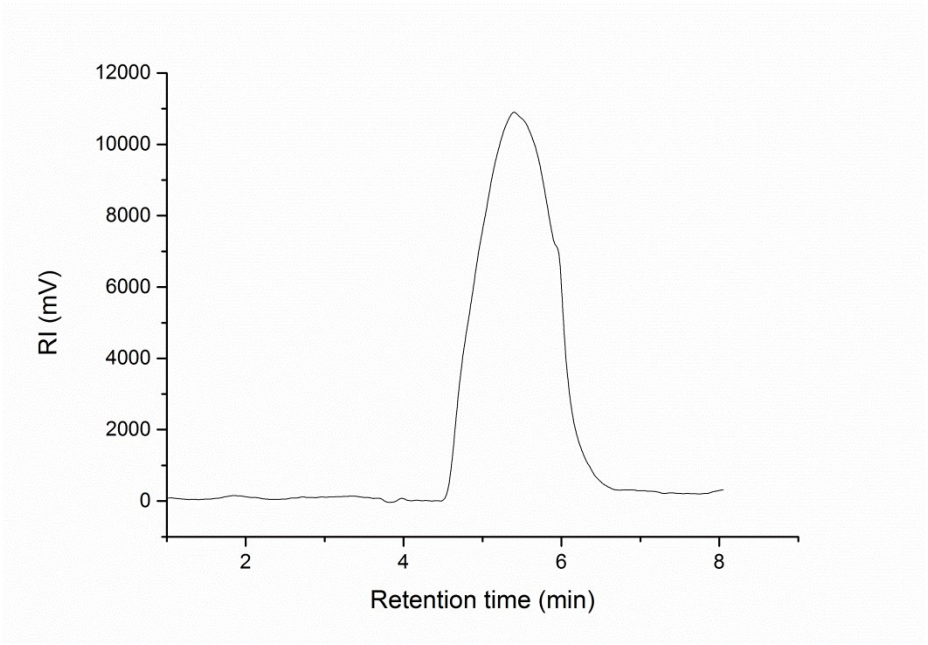

Molecular Weight Averages

Peak	Mp	Mn	Mw	Mz	Mz+1	Mv	PD
Peak 1	972858	601189	1299057	2289610	3183482	2150613	2.161

Figure S39. The GPC of polyisoprene at IP : Fe = 10000:1(Table 1, entry 10)

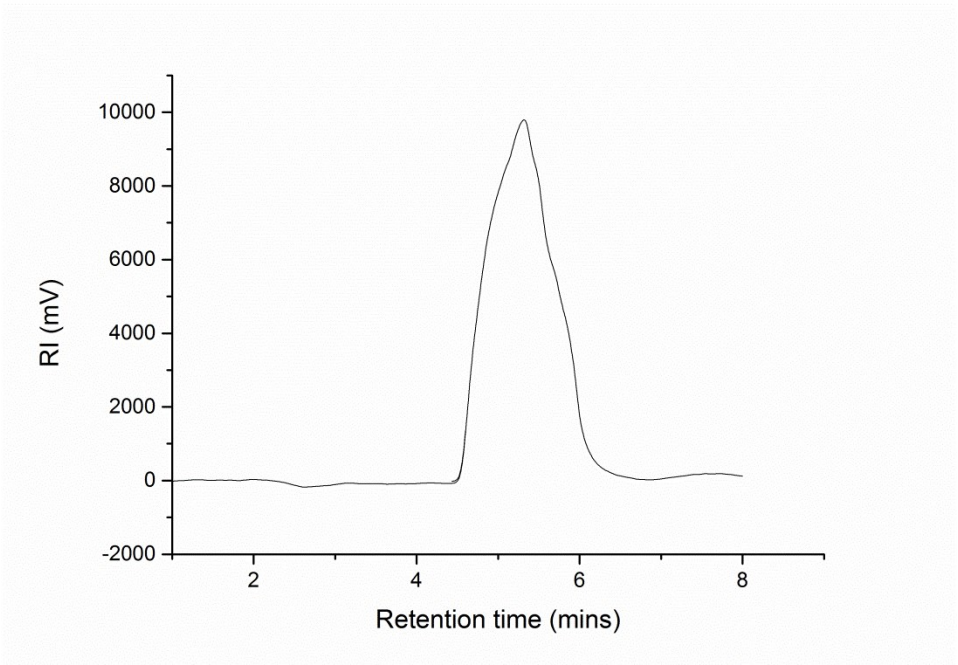

Molecular Weight Averages

Peak	Mp	Mn	Mw	Mz	Mz+1	Mv	PD
Peak 1	1193495	853581	1642648	2607587	3442487	2476141	1.924

Figure S40. The GPC of polyisoprene at IP : Fe = 20000:1(Table 2, entry 11)

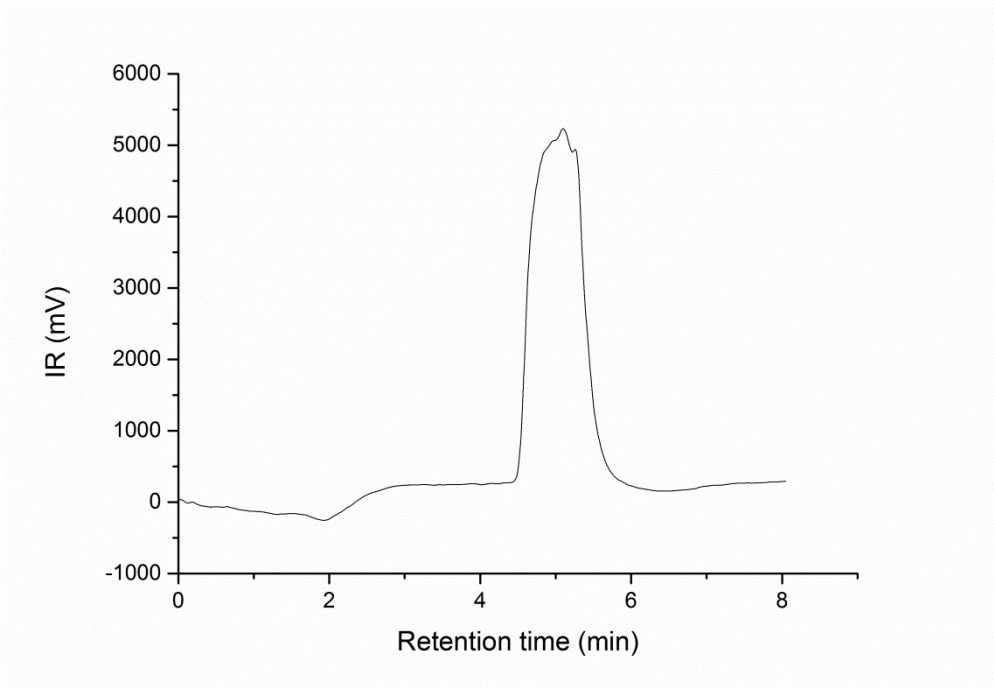

Molecular Weight Averages

Peak	Mp	Mn	Mw	Mz	Mz+1	Mv	PD
Peak 1	1934835	1813956	2581249	3400812	4122416	3287362	1.423

Figure S41. The GPC of polyisoprene at IP : Fe = 200000:1(Table 1, entry 12)

6 X-Ray Crystallography of Complexes

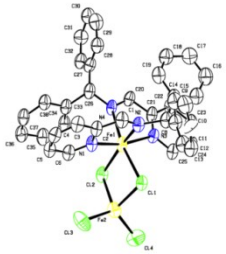

Figure S42 X-Ray Crystallography of Complex **3a**

Fe(II) complex **3a:**

CCDC	1830599
Chemical formula	$C_{38.50}H_{33}Cl_5Fe_2N_4$
M_r	840.64
Crystal system, space group	Orthorhombic, $Pna2_1$
Temperature (K)	298
a, b, c (Å)	25.661 (2), 13.0847 (13), 12.5254 (12)
V (Å^3)	4205.7 (7)
Z	4
Radiation type	Mo $K\alpha$
μ (mm^{-1})	1.04
Crystal size (mm)	0.30 × 0.14 × 0.08
Data collection	
Diffractometer	CCD area detector
Absorption correction	Multi-scan
	SADABS
T_{min}, T_{max}	0.746, 0.922
No. of measured, independent and observed [$I > 2\sigma(I)$] reflections	19963, 7306, 4521
R_{int}	0.101
$(\sin \theta/\lambda)_{max}$ (Å^{-1})	0.595
Refinement	
$R[F^2 > 2\sigma(F^2)]$, $wR(F^2)$, S	0.087, 0.219, 1.10
No. of reflections	7306
No. of parameters	488
No. of restraints	1
H-atom treatment	H atoms treated by a mixture of independent and constrained refinement
$\Delta\rho_{max}$, $\Delta\rho_{min}$ (e Å^{-3})	0.70, −0.40
Absolute structure	Flack H D (1983), Acta Cryst. A39, 876-881
Absolute structure parameter	−0.03 (4)

Fe(II) complex **3d:**

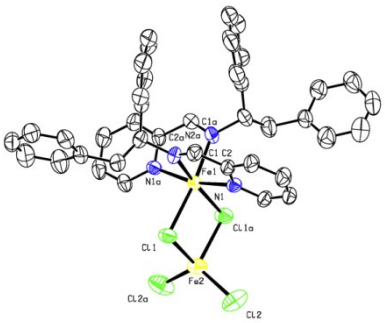

Figure S43 X-Ray Crystallography of Complex **3d**

CCDC	1988978
Crystal data	
Chemical formula	$C_{40}H_{36}Cl_4Fe_2N_4$
M_r	826.23
Crystal system, space group	Monoclinic, *C*2/*c*
Temperature (K)	298
a, *b*, *c* (Å)	23.531 (2), 13.9550 (11), 15.0761 (13)
β (°)	129.840 (4)
V (Å^3)	3801.2 (6)
Z	4
Radiation type	Mo *K*α
μ (mm^{-1})	1.08
Crystal size (mm)	0.15 × 0.10 × 0.04
Data collection	
Diffractometer	CCD area detector
Absorption correction	Multi-scan *SADABS*
T_{min}, T_{max}	0.855, 0.958
No. of measured, independent and observed [$I > 2\sigma(I)$] reflections	8343, 3300, 1495
R_{int}	0.127
$(\sin \theta/\lambda)_{max}$ (Å^{-1})	0.595
Refinement	
$R[F^2 > 2\sigma(F^2)]$, $wR(F^2)$, S	0.094, 0.240, 1.05
No. of reflections	3300
No. of parameters	227
H-atom treatment	H atoms treated by a mixture of independent and constrained refinement
$\Delta\rho_{max}$, $\Delta\rho_{min}$ (e Å^{-3})	0.58, −0.85

7. Mössbauer spectrum of Complexes

Fe(II) complex **3b:**

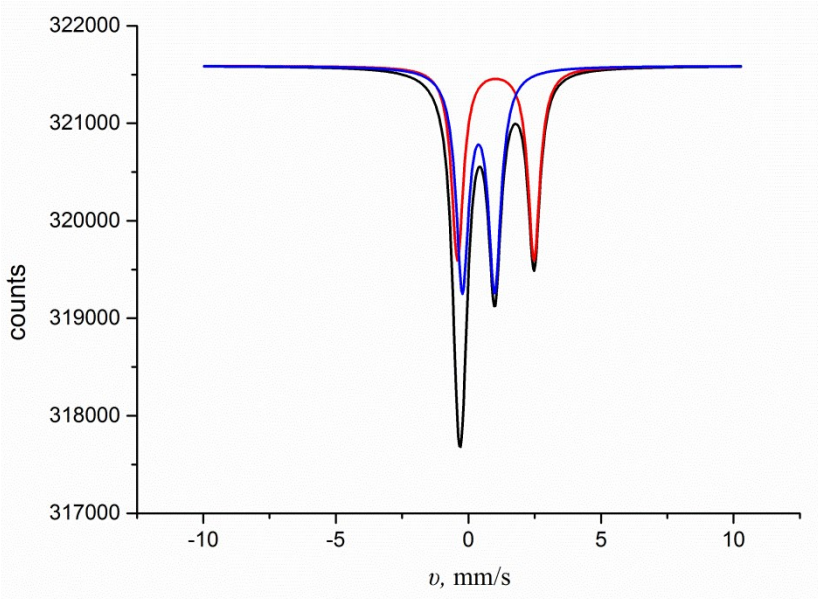

Figure S44 Mössbauer spectrum of complex **3b**

Zero-field Mössbauer spectrum of unsymmetric diiron complex **3b** fit as a pair of quadrupolar doublets, with δ = 1.03 mm s^{-1}, ΔEQ = 2.88 mm s^{-1} (red line, doublet 1 fit) and δ = 0.38 mm s^{-1}, ΔEQ = 1.22 mm s^{-1} (blue line, doublet 2 fit). The total fit is shown as a black line.

Fe(II) complex **3c:**

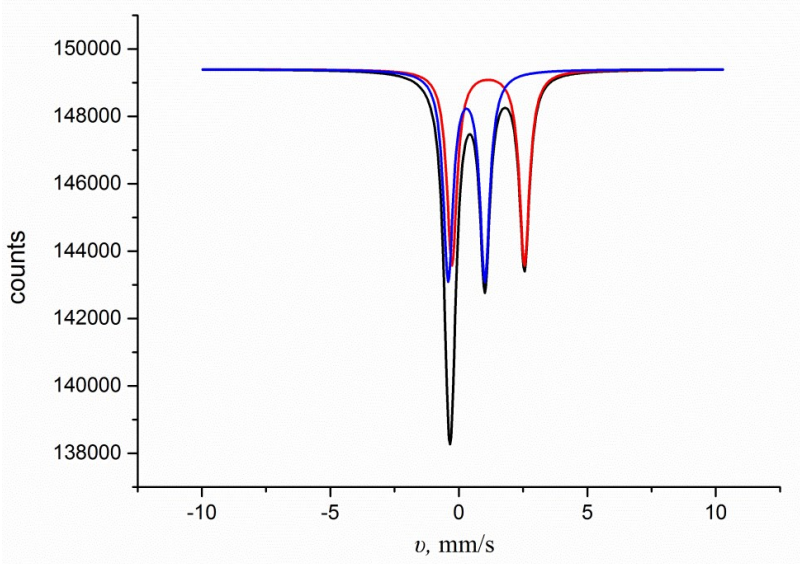

Figure S45 Mössbauer spectrum of complex **3c**

Zero-field Mössbauer spectrum of unsymmetric diiron complex **3c** fit as a pair of quadrupolar doublets, with δ = 1.14 mm s^{-1}, ΔEQ = 2.82 mm s^{-1} (red line, doublet 1 fit) and δ = 0.30 mm s^{-1}, ΔEQ = 1.42 mm s^{-1} (blue line, doublet 2 fit). The total fit is shown as a black line.

8. Mechanical properties of synthetic poyisoprene and natural rubber

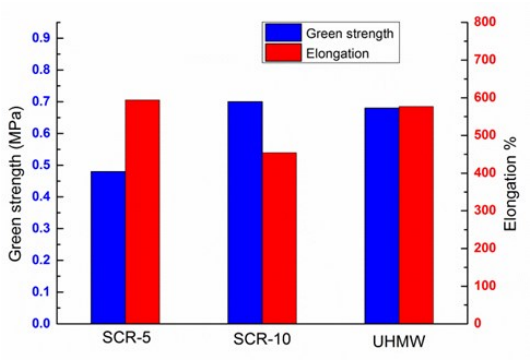

Figure S46 Comparison of mechanical properties of uncross-link synthetic polymers produced by complex **3a** and natural rubber

9. The transition glass temperatures (Tg) of the various polymers

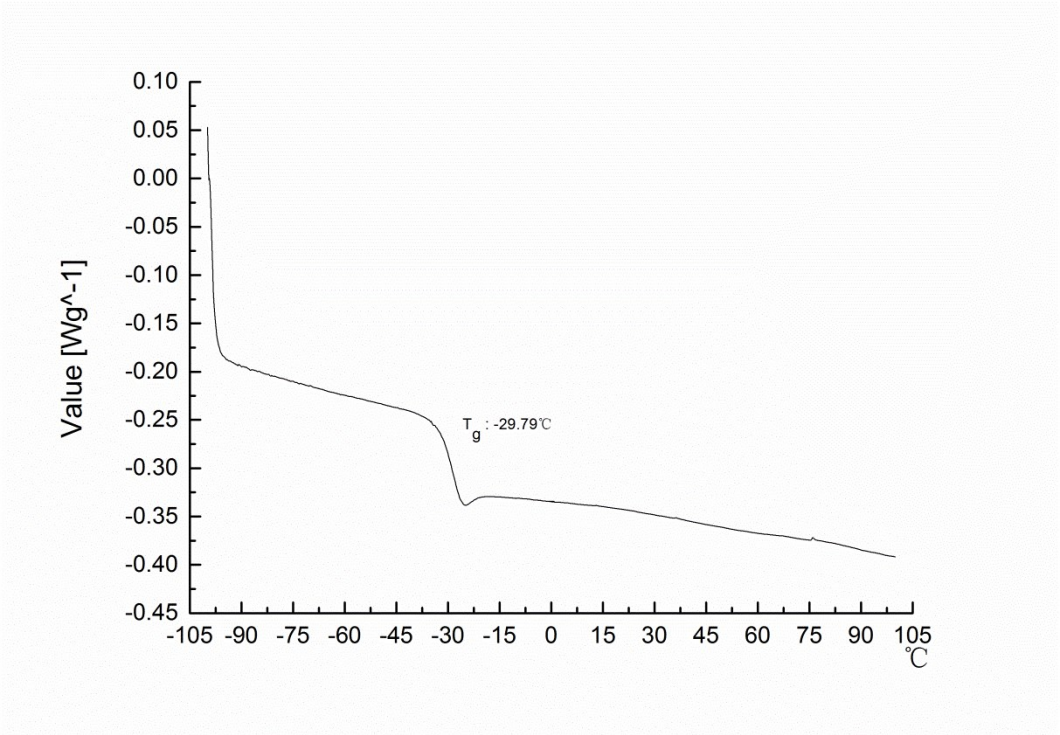

Figure S47 The transition glass temperatures (T_g) of Table 1, entry 1

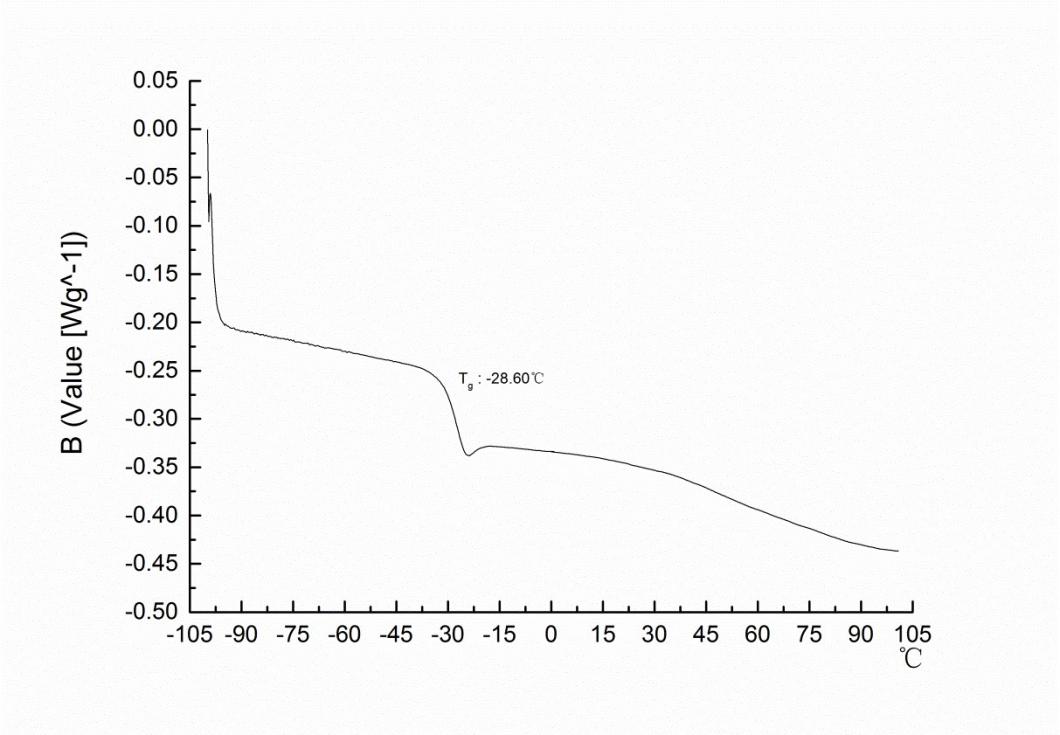

Figure S48 The transition glass temperatures (T_g) of Table 1, entry 6

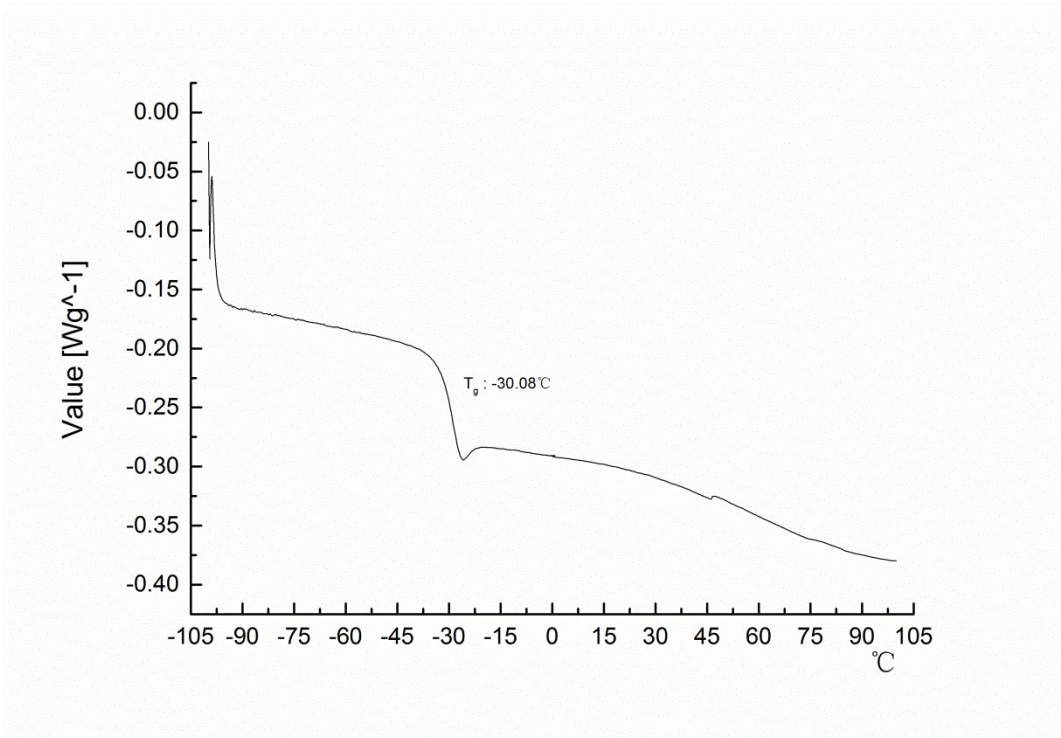

Figure S49 The transition glass temperatures (T_g) of Table 1, entry 7

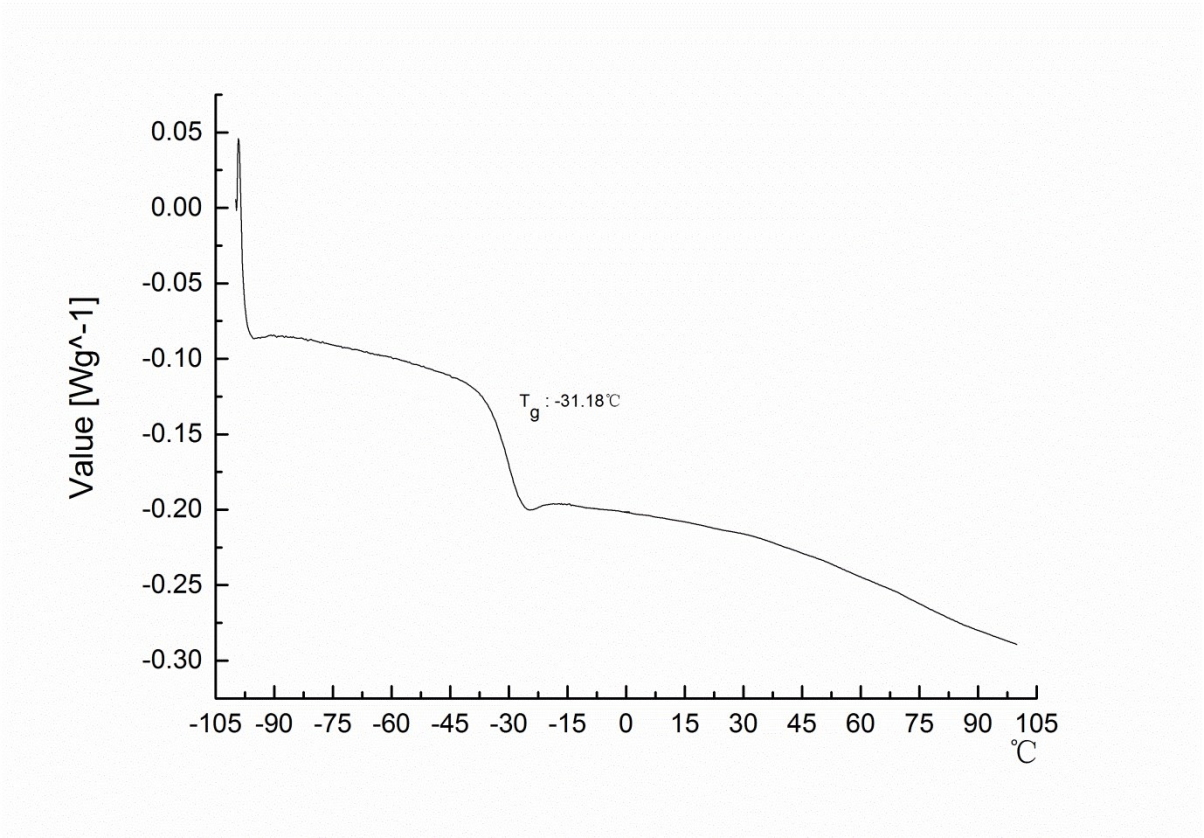

Figure S50 The transition glass temperatures (T_g) of Table 1, entry 8

10. Distribution of the various monomeric units along the polymer chain.

Table Polyisoprene ^{13}C NMR signal assignments [ref. 1]

Carbon atom	signal	Assignment	Chemical shift (Obs.(ref 1))
3	A	c-V-c,t	47.79
	B	t-V-c,t	47.07
	C	c,t-V-v & v-V-c,t	45.35
	D	v-V-v	41.98
1	E	c-T	38.86
	F	t-T	39.70
	H	v-T	37.39
	J	c-C	32.08
	K	t-C	31.95
	M	v-C	29.88
4	G	V-v(m)	37.55
	I	V-v(r)	32.67
	J	T-v	32.08
	K	T-v	31.95
	L	C-v	31.33
		V-c	31.33
	N	V-t	28.21
	O	T-c,t	26.36
	O	C-c,t	26.69
5	P	C	23.25
	Q	c,t-V-c,t	18.74
	R	c,t-V-V	18.04
		V-V-c,t	18.04
	S	V-V-V	17.58
	T	T	15.76

Sequence distribution of *cis-1,4, trans-1,4,* and 3,4-units

Sequence	**Method**
Cis-trans	E/∑
Trans-trans	F/∑
3,4-*trans*	H/∑
Cis-cis	(J+K-N)/∑
Trans -cis	

3,4-*cis*	M/∑
Cis-3,4-1,4	A/∑
Trans-3,4-1,4	B/∑
1,4-3,4-3,4	C/∑
3,4-3,4-1,4	
3,4-3,4-3,4	D/∑

Calculated values were obtained on the assumption of a random distribution of the isomeric units using the fractions of these units from the relative intensities of C1 and C3 carbon signals

∑: A +B +C +D +E +F +H +J +K+M-N and 1,4 = *cis* or *trans*.

Reference:

1 H. Sato, A. Ono and Y. Tanaka, *Polymer* **1977**, 18, 580−586.

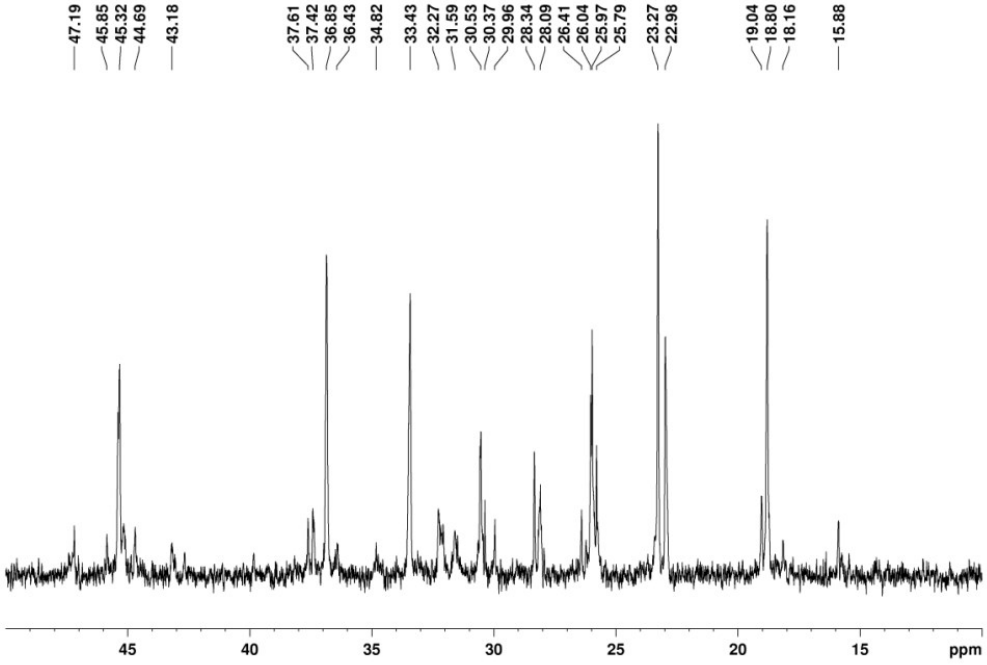

Figure S51. Sequence distribution of *cis-1,4, trans-1,4,* and 3,4-units (Table 1, entry 1)

Table Polyisoprene ^{13}C NMR signal assignments

signal	Assignment	Chemical shift		Content
		Obs.(ref)	Obs.	
A	c-V-c,t	47.79	--	--
B	t-V-c,t	47.07	47.19	0.068
C	c,t-V-v & v-V-c,t	45.35	45.32	0.5533
D	v-V-v	41.98	--	--
E	c-T	38.86	--	--
F	t-T	39.70	--	--
H	v-T	37.39	37.42	0.107
J	c-C	32.08	32.27	0.265
K	t-C	31.95	--	--
M	v-C	29.88	29.95	0.071
N	V-t	28.21	28.34	0.129
∑	A +B +C +D +E +F +H +J +K+M-N	---	--	0.9353

Sequence distribution of *cis-1,4, trans-1,4,* and 3,4-units

Sequence	**Method**	**Result**
Cis-trans	E/∑	0
Trans-trans	F/∑	0

3,4-*trans*	H/∑	11
Cis-cis	(J+K-N)/∑	15
Trans -cis		
3,4-*cis*	M/∑	8
Cis-3,4-1,4	A/∑	0
Trans-3,4-1,4	B/∑	7
1,4-3,4-3,4	C/∑	59
3,4-3,4-1,4		
3,4-3,4-3,4	D/∑	0

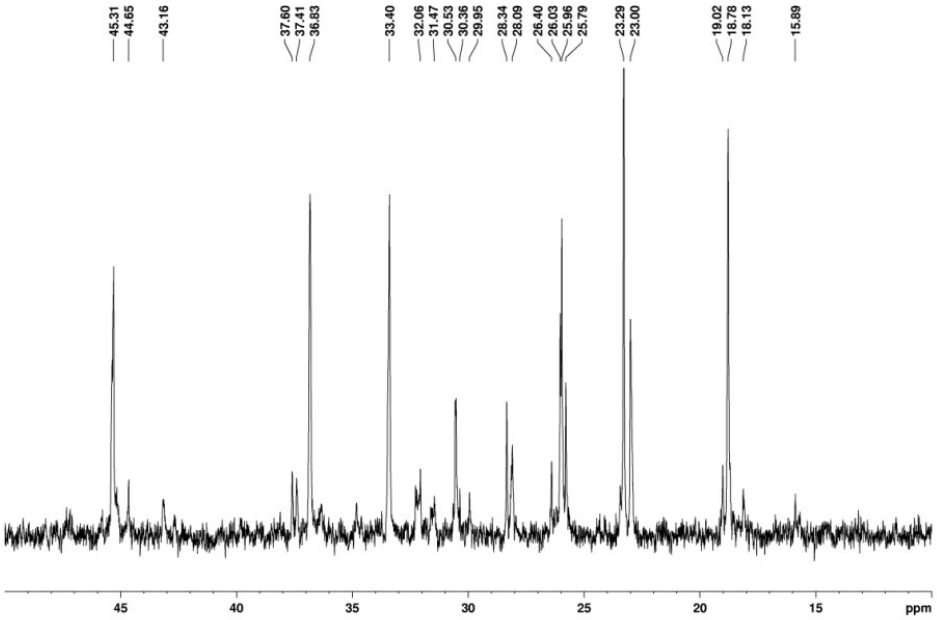

Figure S52. Sequence distribution of *cis-1,4, trans-1,4,* and 3,4-units (Table 1, entry 6)

Table Polyisoprene ^{13}C NMR signal assignments

signal	Assignment	Chemical shift		Content
		Obs.(ref)	Obs.	
A	c-V-c,t	47.79	--	--
B	t-V-c,t	47.07	--	--
C	c,t-V-v & v-V-c,t	45.35	45.31	0.5846
D	v-V-v	41.98	--	--
E	c-T	38.86	--	--
F	t-T	39.70	--	--
H	v-T	37.39	37.41	0.0784
J	c-C	32.08	32.06	0.1763
K	t-C	31.95	--	--
M	v-C	29.88	29.95	0.0444
N	V-t	28.21	28.34	0.1195
∑	A +B +C +D +E +F +H +J +K+M-N			0.7642

Sequence distribution of *cis-1,4, trans-1,4,* and 3,4-units

Sequence	**Method**	**Result**
Cis-trans	E/∑	0
Trans-trans	F/∑	0
3,4-*trans*	H/∑	10

Cis-*cis*	(J+K-N)/∑	7
Trans -*cis*		
3,4-*cis*	M/∑	6
Cis-3,4-1,4	A/∑	0
Trans-3,4-1,4	B/∑	0
1,4-3,4-3,4	C/∑	77
3,4-3,4-1,4		
3,4-3,4-3,4	D/∑	0

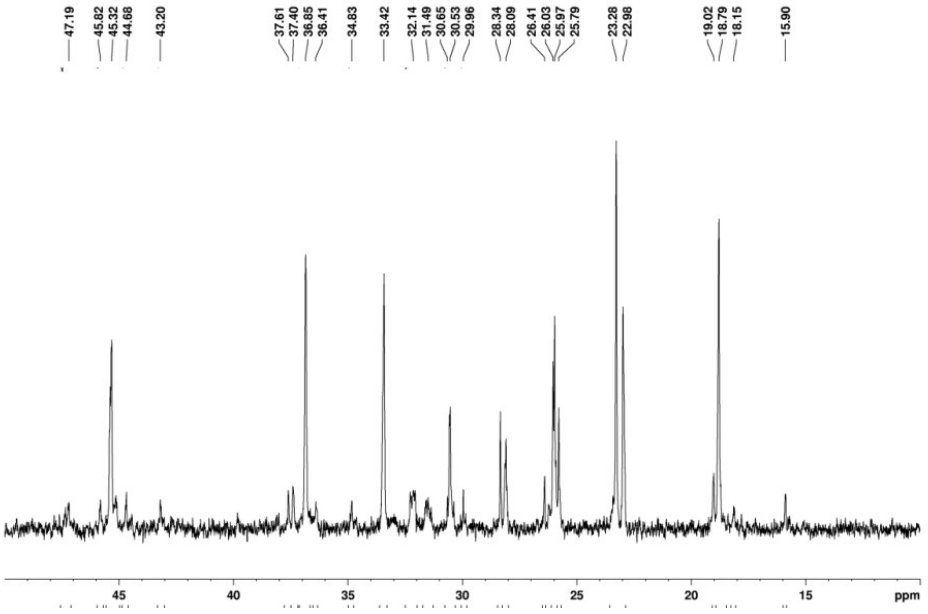

Figure S53. Sequence distribution of *cis-1,4, trans-1,4,* and 3,4-units (Table 1, entry 7)

Table Polyisoprene 13C NMR signal assignments

signal	Assignment	Chemical shift		Content
		Obs.(ref)	Obs.	
A	c-V-c,t	47.79	--	--
B	t-V-c,t	47.07	47.19	0.0514
C	c,t-V-v & v-V-c,t	45.35	45.32	0.552
D	v-V-v	41.98	--	--
E	c-T	38.86	--	--
F	t-T	39.70	--	--
H	v-T	37.39	37.40	0.0913
J	c-C	32.08	32.14	0.197
K	t-C	31.95	--	--
M	v-C	29.88	29.96	0.0553
N	V-t	28.21	28.34	0.1298
∑	A +B +C +D +E +F +H +J +K+M-N	--	--	0.8172

Sequence distribution of cis-1,4, trans-1,4, and 3,4-units

Sequence	Method	Result
Cis-trans	E/∑	0
Trans-trans	F/∑	0
3,4-*trans*	H/∑	11

Cis-*cis*	(J+K-N)/∑	8
Trans -*cis*		
3,4-*cis*	M/∑	7
Cis-3,4-1,4	A/∑	0
Trans-3,4-1,4	B/∑	6
1,4-3,4-3,4	C/∑	68
3,4-3,4-1,4		
3,4-3,4-3,4	D/∑	0

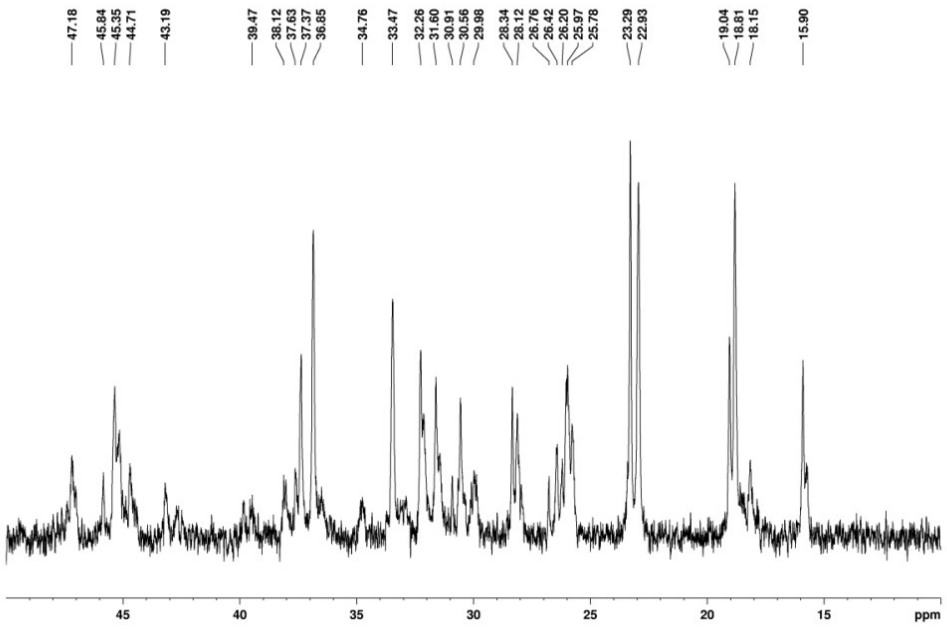

Figure S54. Sequence distribution of *cis-1,4, trans-1,4,* and 3,4-units (Table 1, entry 8)

Table Polyisoprene ^{13}C NMR signal assignment

signal	Assignment	Chemical shift		Content
		Obs.(ref)	Obs.	
A	c-V-c,t	47.79	--	--
B	t-V-c,t	47.07	47.18	0.212
C	c,t-V-v & v-V-c,t	45.35	45.35	0.4499
D	v-V-v	41.98	--	--
E	c-T	38.86	--	--
F	t-T	39.70	--	--
H	v-T	37.39	37.37	0.2509
J	c-C	32.08	32.26	0.4245
K	t-C	31.95	--	--
M	v-C	29.88	29.98	0.1835
N	V-t	28.21	28.34	0.1439
∑	A +B +C +D +E +F +H +J +K+M-N	--	--	1.3769

Sequence distribution of *cis-1,4, trans-1,4,* and 3,4-units

Sequence	**Method**	**Result**
Cis-trans	E/∑	0
Trans-trans	F/∑	0
3,4-*trans*	H/∑	18

Cis-cis	(J+K-N)/∑	20
Trans -cis		
3,4-*cis*	M/∑	13
Cis-3,4-1,4	A/∑	0
Trans-3,4-1,4	B/∑	16
1,4-3,4-3,4	C/∑	33
3,4-3,4-1,4		
3,4-3,4-3,4	D/∑	0